PERFORMANCE OF REINFORCING STEEL COATED

WITH A HIGH RATIO ZINC SILICATE

by

ROBERT JOSEPH FROSCH, B.S.E.

THESIS

Presented to the Faculty of the Graduate School of

The University of Texas at Austin

in Partial Fulfillment

of the Requirements

for the Degree of

MASTER OF SCIENCE IN ENGINEERING

THE UNIVERSITY OF TEXAS AT AUSTIN

December 1992

ACKNOWLEDGEMENTS

Robert Joseph Frosch
November 18, 1992

TABLE OF CONTENTS

LIST OF TABLES

LIST OF FIGURES

CHAPTER 1

INTRODUCTION

1.1 Reinforcing Steel Corrosion

Corrosion of reinforcing steel in concrete is a problem that threatens the integrity of structures and shortens their service life. The problems can range from aesthetic (concrete staining) to severe structural deterioration. Structural problems include a reduction in steel cross-sectional area and loss of concrete cover. The severity of these problems could lead to a structural failure.

Reinforcement may corrode wherever structural elements are exposed to the weather or to other environments which may attack the materials in reinforced concrete structures. Accelerated corrosion can be expected for structures in marine environments, in industrial or manufacturing environments where corrosive chemicals are used, and in deicing salt environments. The latter exposure condition is common for northern bridge decks and parking structures. Parking garages have shown severe corrosion due to the high concentrations of deicing salts transported by vehicles.

Corrosion can be delayed or prevented by improving the concrete quality to decrease permeability, increasing the concrete cover, applying waterproofing membranes, and protecting the reinforcement. The primary means of reinforcement protection used today is epoxy-coated reinforcement. An epoxy coating is usually fusion-bonded to the steel to prevent water and salts from reaching the steel and to electrically isolate the reinforcement.

1

1.2 Corrosion of Reinforcement in Concrete

Corrosion of reinforcement is an electrochemical process and is shown schematically in Figure 1.1. An electrical connection carries electrons from the anode to the cathode while anions are carried in the reverse direction through a salt bridge. The basic reactions for the cathode and anode are also given in the figure. Corrosion can occur in the presence of oxygen and water, but steel is normally protected by an oxide film that exists on the surface. Chlorides, however, can assist and accelerate the corrosion process. Chloride ions act to break down the oxide coating and open a path for water and oxygen to reach the steel.

Anode: $2 [Fe_{(s)} \rightarrow Fe^{2+}_{(aq)} + 2e^-]$

Cathode: $O_2 + 2H_2O + 4e^- \rightarrow 4OH^-_{(aq)}$

Net: $2Fe_{(s)} + O_2 + 2H_2O \rightarrow 2Fe(OH)_2$
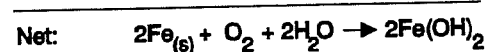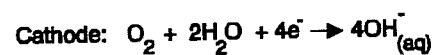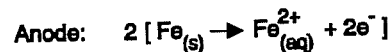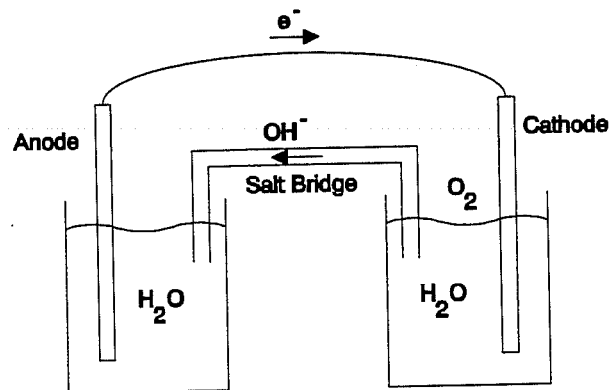
Figure 1.1: Electrochemical Corrosion

Corrosion of reinforcement in concrete can occur by either macrocell or microcell action. Both methods involve the same corrosion processes as discussed above. Microcell corrosion acts on one piece of steel where sections become anodes and the rest of the bar becomes the cathode as shown in Figure 1.2(a). The anode is created if there is a
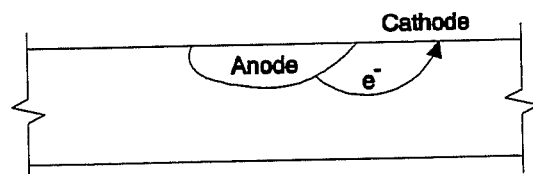
Figure 1.2: Microcell Corrosion

break in the oxide coating; the electron transfer occurs internally through the steel.

Macrocell action occurs by a galvanic cell being set up within the concrete member. The cell can be set up in structural members and systems such as a bridge deck shown in Figure 1.2(b). In macrocell action, the cathode and anode are separated. The top mat of reinforcement becomes the anode while the bottom mat becomes the cathode. The electrical connection is achieved by stirrups which connect the mats together for the transfer of electrons. The salt bridge is formed by the moist concrete which is
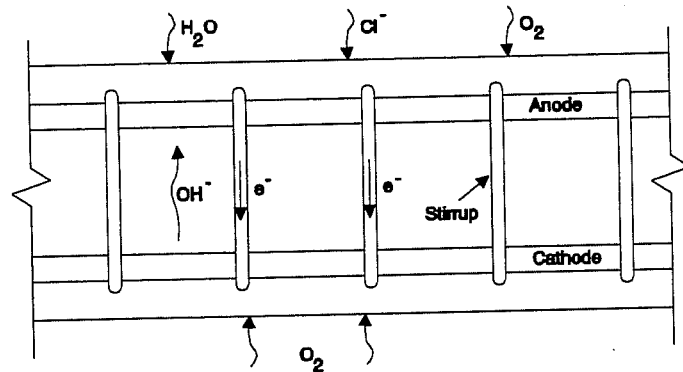
Figure 1.3: Macrocell Corrosion

called the electrolyte. Water, oxygen, and chlorides from deicing salts are sufficient ingredients for corrosion to initiate.

Corrosion protection can be achieved through the use of coatings. The anode can be protected or covered to prevent both microcell and macrocell action. An example is epoxy-coated reinforcement which prevents water and chlorides from reaching the steel. Another method is cathodic protection which forces another metal to become the anode while the steel is converted to a cathode. An example of a sacrificial anode is a zinc coating.

1.3 Structural Problems of Coatings

The use of coatings to eliminate corrosion have a potential for creating structural problems. Coatings place a foreign material at the interface

between the concrete and steel which can effect the bond and bond strength. Epoxy coating eliminates adhesion of the concrete to the bar and reduces friction. These effects increase the splitting stresses which in turn decrease the bond strength of reinforcement for splitting type failures. Splitting is the most common bond failure mode due to the use of small concrete covers and reinforcement spacings. The decrease in bond strength is not as pronounced with pull-out failures since failure is due to shearing of the concrete by the steel deformations. Due to the decreased bond strength, the development length must be increased. Provisions have been made in ACI 318-89[1] Section 12.2.4.3 for increasing the development and splice lengths of epoxy-coated reinforcement. The lengths are increased by 50 percent for small covers and spacings (covers $< 3d_b$ or clear spacing $< 6d_b$) and 20 percent for large covers and spacings.

Another structural problem evident from epoxy-coated reinforcement is that the coating increases crack widths while decreasing the number of cracks. This effect must be considered if cracking and crack widths are important such as in water containment structures. In addition, larger cracks can allow more corrosive material to reach the reinforcement.

Since coatings can have an influence on bond and the general behavior of a structural element, the effects of any coating on the structural properties of reinforced concrete sections and members must be evaluated.

1.4 Objective and Scope

The objective of the research performed in this study was to evaluate the structural performance and corrosion characteristics of reinforcing steel coated with a high ratio zinc silicate. Two separate studies were conducted: tests of beams with spliced bars to determine the bond characteristics of the coated

bars and macrocell tests to investigate the protection afforded by a high ratio zinc silicate coating to reinforcement in a corrosive environment.

CHAPTER 2

STRUCTURAL BOND - EXPERIMENTAL PROGRAM

2.1 Introduction

Eight beams were tested to compare the bond strength of spliced reinforcing bars coated with a high ratio zinc silicate to the bond strength of uncoated reinforcing steel. The influence of the coating on stiffness and crack-width was also investigated.

2.2 Design of Specimens

Beams were designed to permit comparisons with previous tests[17] performed for determining bond strength of epoxy coated reinforcing bars. The loading system was designed to produce a constant moment region in the center portion of the specimen where the splice is located (Figure 2.1). The test arrangement provides the most severe condition on the lap splice since the total tension in the reinforcement is constant across the entire constant moment region. The specimens were tested in negative bending for the convenience of observation and for the ease in measuring the crack widths during testing.

Tests were performed on two different reinforcing bar sizes, #6 and #11. These two sizes were chosen since they bracket the range of the most common bar sizes used as primary reinforcement. Bridge decks are commonly reinforced with #6 bars while #11 bars are the largest bars normally used for flexural or compression members.

The splices were designed so that the reinforcement would not reach yield prior to bond failure. If the bars yield, a comparison of bond strengths can not be made. An 18 inch splice length was chosen for the #6 bar specimens

while a 36 inch splice was chosen for the #11 bar specimens. The reinforcement in the ends of the beam was well anchored.

Side Elevation

End Elevation
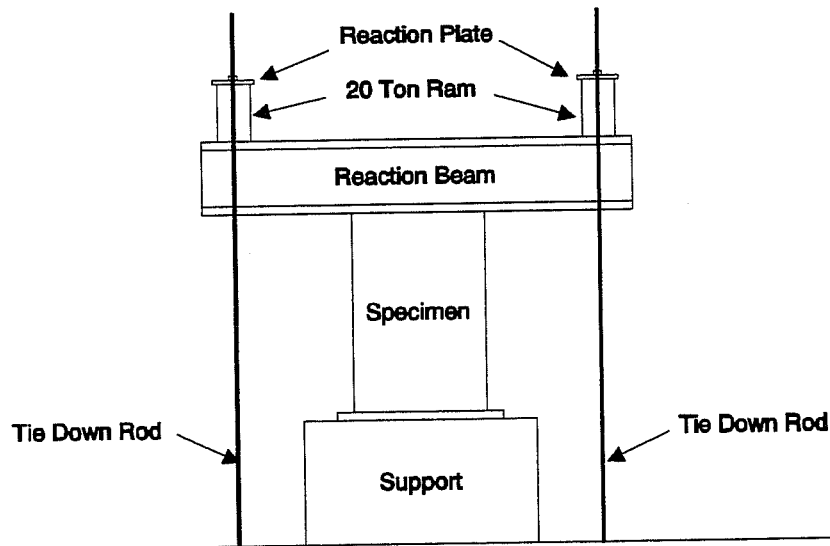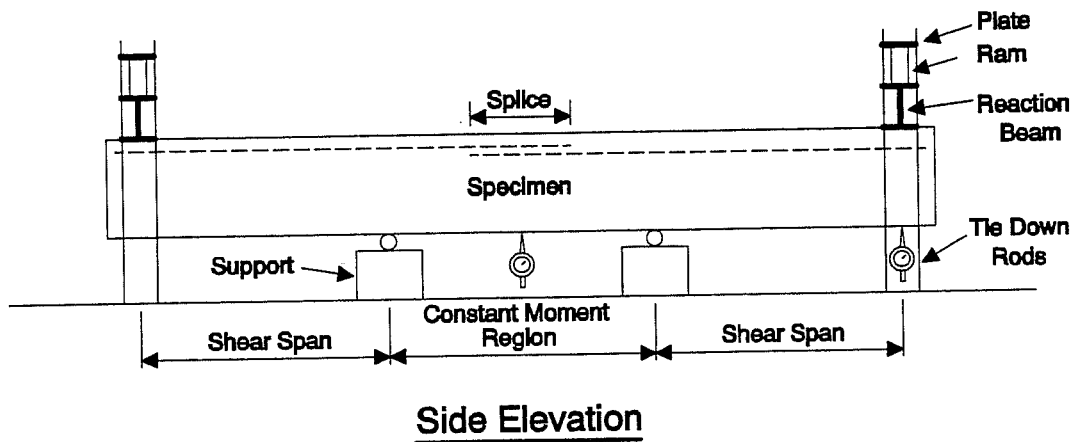
Figure 2.1: Loading System

The beam lengths were determined to accommodate the splice lengths selected and to meet the restraints imposed by the dimensions of the reaction

floor at the Ferguson Structural Laboratory. Since the tie-down anchors are spaced at four foot intervals in all directions, the distance between loading points must also be in four foot intervals. In addition to this constraint, the cracking behavior needed to be considered in order to provide for measuring crack widths. A crack will usually occur at the ends of the splice and directly over the supports. In measuring the spacing and widths of cracks, it is important to have a sufficient length between the support and the end of the splice for a random distribution of cracking to occur.

To satisfy the constraints mentioned above, the specimens with #6 bars were designed with a 4 ft. constant moment region and a 12 ft. span between loading points. Six inches were added to each end to accommodate the loading beam. The total beam length was 13 ft. as shown in Figure 2.2. The
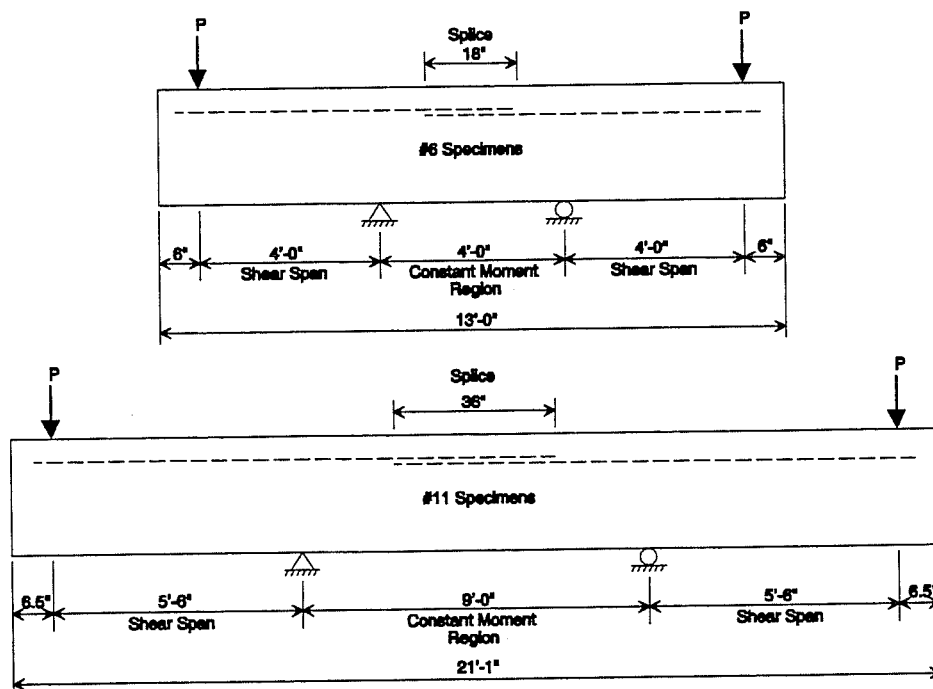
Figure 2.2: Beam Dimensions

specimens with #11 bars were designed with a 9 ft. constant moment region and a 20 ft. span between loading points. In order to accommodate the loading beam, 6.5 inches were added to each end. The total beam length was 21 ft. - 1 in. as shown in Figure 2.2.

The beam cross-sections are shown in Figure 2.3. The total beam depth for all specimens was 16 inches. This dimension was used to allow the reinforcement to be cast in the top position (more than 12 inches of fresh

(a): Series 1

(b): Series 2

Figure 2.3: Cross Sections
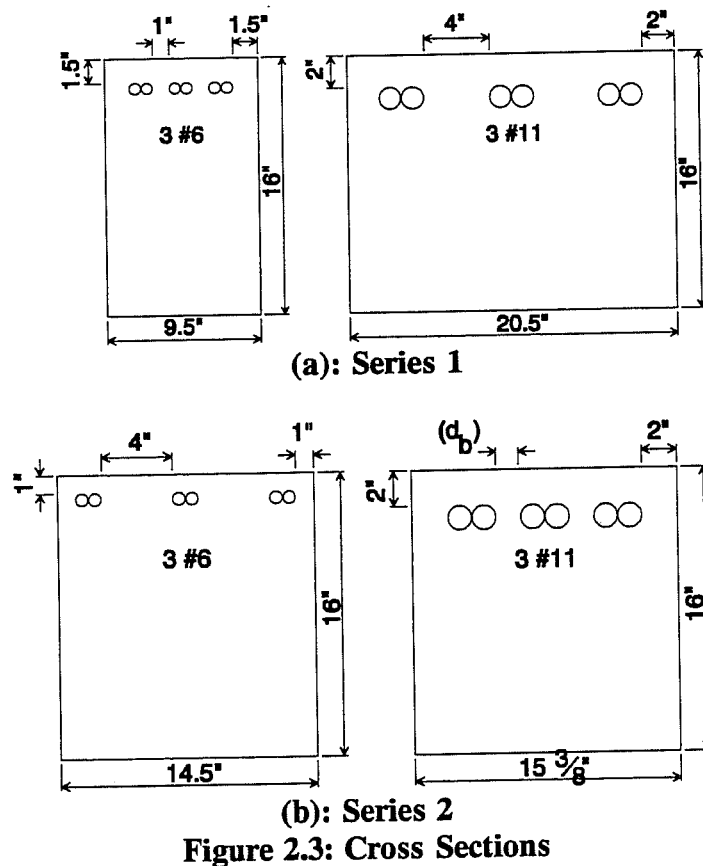
concrete cast in the member below the reinforcement). The beam depth also corresponds to that used in previous tests.[17] The actual cover and spacing

dimensions of each specimen are tabulated in Appendix A. The constructed dimensions were very close to the design values.

The width of the specimens was determined by the selected cover and spacing dimensions. For the #11 specimens, the cover was set at 2 inches which corresponds with the minimum cover required by ACI 318-89[1] for concrete exposed to earth or weather and with the recommendations for corrosive environments. In addition, the cover corresponds with AASHTO[2] requirements. The clear separation was varied for the two series of tests. Series 1 included a 4 inch spacing since this dimension will produce either a side split failure or a face and side split failure (Figure 2.4).[14] In Series 2, a one bar diameter (d_b) spacing was used since this is the minimum spacing allowed by the ACI code.
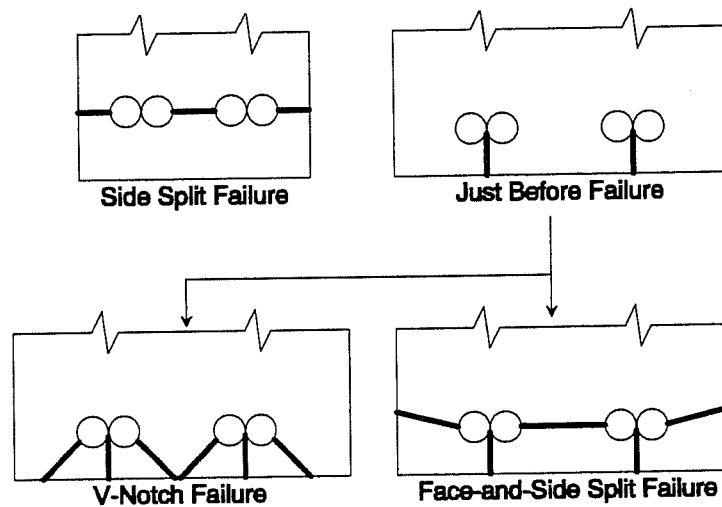
Figure 2.4: Splitting Failure Modes

For the #6 specimens, the cover was decreased to ensure that the splice would fail before reaching yield. Series 1 included a 1.5 inch cover with a 1 inch spacing. The spacing is the minimum allowed by the ACI code and the

cover corresponds with the minimum cover for concrete not exposed to weather or in contact with ground. In the Series 2 tests, the cover was further reduced to 1 inch to study the effects of a small cover and wide spacing between bars which would be more likely to fail in face splitting.

A summary of the specimen details is given in Table 2.1. The specimens are identified by the initial of the reinforcement type (Black or Coated) followed by the Series number and by the bar size (#6 or #11). As an example, B1-6 identifies a Series 1 specimen with #6 black (uncoated) bars.

Table 2.1: Details of Beams with Lap-Splices					
Specimen	Bar		Splice Length, l_s (in.)	Cover (in.)	Spacing (in.)
	Type	Size			
B1-6	Black	#6	18	1.5	1.0
C1-6	Coated	#6	18	1.5	1.0
B1-11	Black	#11	36	2.0	4.0
C1-11	Coated	#11	36	2.0	4.0
B2-6	Black	#6	18	1.0	4.0
C2-6	Coated	#6	18	1.0	4.0
B2-11	Black	#11	36	2.0	1.410
C2-11	Coated	#11	36	2.0	1.410

2.3 Materials

2.3.1 Reinforcing Steel

The reinforcing steel (coated and uncoated) used for the primary reinforcement was obtained from the coating supplier. Both #6 and #11 bars

were Grade 60 and had a diamond deformation pattern. All bars of a given size were obtained from the same heat of steel to insure that both the chemical and mechanical properties of the bars were identical. To eliminate variations, it is important that companion specimens with coated and uncoated bars have identical deformations. A tension test of a #6 and #11 bar indicated a yield strength of 61,250 psi and 73,500 psi respectively.

Reinforcement required for stirrups and bottom longitudinal reinforcement was obtained from a different supplier. Grade 60, #3 bars were used for these purposes.

The coated steel arrived in good condition with only small abrasions from transportation. The average thickness of the coating measured with a dry film thickness gage (Category - Type 1 magnetic pull-off) was 4 mils.

2.3.2 Concrete

The concrete was obtained from a ready-mix supplier. All specimens were cast using the same mix design, a nominal 4000 psi mix. The mix proportions are shown below. All aggregate weights are for saturated surface dry conditions.

Cement (Type I)	400 pcy
Coarse Aggregate	1862 pcy
Fine Aggregate	1422 pcy
Water	267 pcy
Water Reducer-Retarder	14 ozcy

The actual proportions delivered varied slightly and were adjusted according to the moisture content of the aggregates.

All beams in a series were cast from the same batch of concrete. The first series of beams had a slump of 8 inches while the second series had a slump of 7.5 inches. Standard compression tests of three 6 by 12 inch

cylinders were used to determine average compressive strengths. The strength gain curves of both series of specimens are given in Figure 2.5.
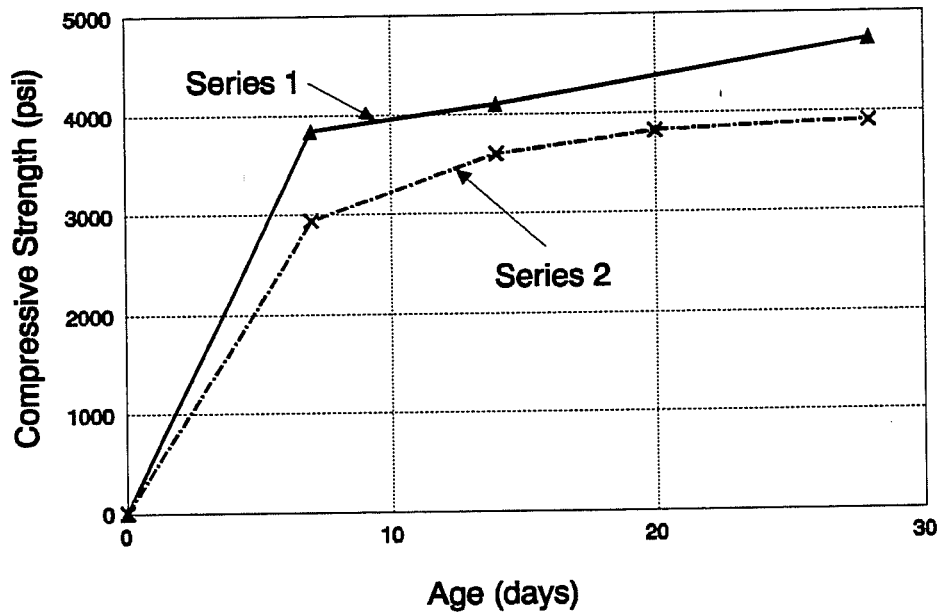
Figure 2.5: Concrete Strength Gain

Split cylinder tests of three 6 by 12 inch cylinders were used to determine the average tensile strength of the concrete. These tests were performed to coincide with the beam tests. The strengths are given below with the respective concrete age.

Series	Age (days)	Tensile Strength (psi)
1	28	.380
2	20	350

2.4 Construction of Specimens

2.4.1 Formwork

The formwork was designed so that two companion specimens could be built side by side to ensure that both specimens were constructed and cast using the same procedures. Two sets of forms were constructed to accommodate two #6 specimens and two #11 specimens and to allow all beams of one series to be cast together. The formwork is shown in Figure 2.6.
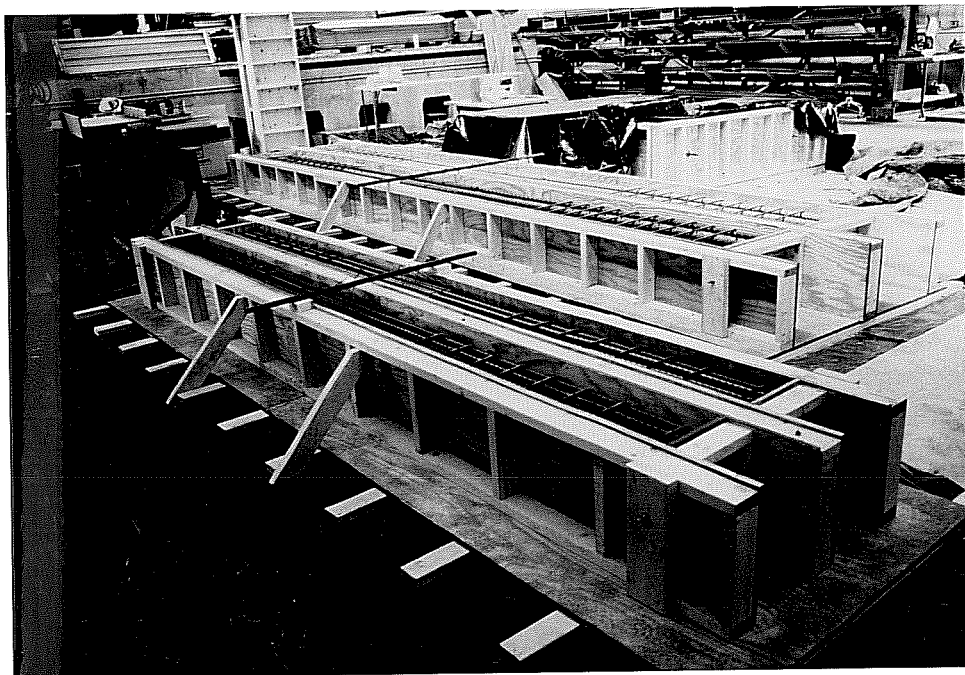
Figure 2.6: Formwork

The forms were constructed with a plywood base of sufficient width that the different width beams of Series 1 and Series 2 could be accommodated. A center divider was fastened to the base with threaded rods that were placed through the center and secured by nuts. The outside forms were attached to

the base by bolts and could be moved in or out to vary the width of the beams. The end forms were attached in the same manner with the addition of a threaded rod that clamped the outer forms together. Braces were included on the sides of the forms to maintain consistent dimensions during casting. This method of attaching the outside and end forms allowed for easy stripping and cleaning of the formwork.

The forms were completed by sealing the joints with a silicone sealer and coating the surfaces with a form release agent.

2.4.2 Fabrication of Cages

The steel cages were fabricated outside the forms and lifted into position. Due to the size of the #11 cages, they were constructed in halves and placed to create the splice within the forms. The cages were seated on individual chairs to provide the correct position in the form.

Closed stirrups were used in the shear span to prevent a shear failure during testing. No stirrups, however, were used in the splice region in order to eliminate the influence of transverse reinforcement on bond strength. Transverse reinforcement in the splice region increases bond strength when a splitting mode of failure controls. Steel reinforcement details are shown in Figure 2.7. Two #3 bars were used as bottom steel for the entire length of all specimens to help hold the cages together and maintain the steel dimensions in the forms.

Since stirrups were not used in the splice region, the bars needed to be held in place by a rod placed across the width of the forms as shown in Figure 2.8. Tie wires were used to hold the splices in position. This procedure permitted adjustment of cover and spacing dimensions to achieve the values selected in design.
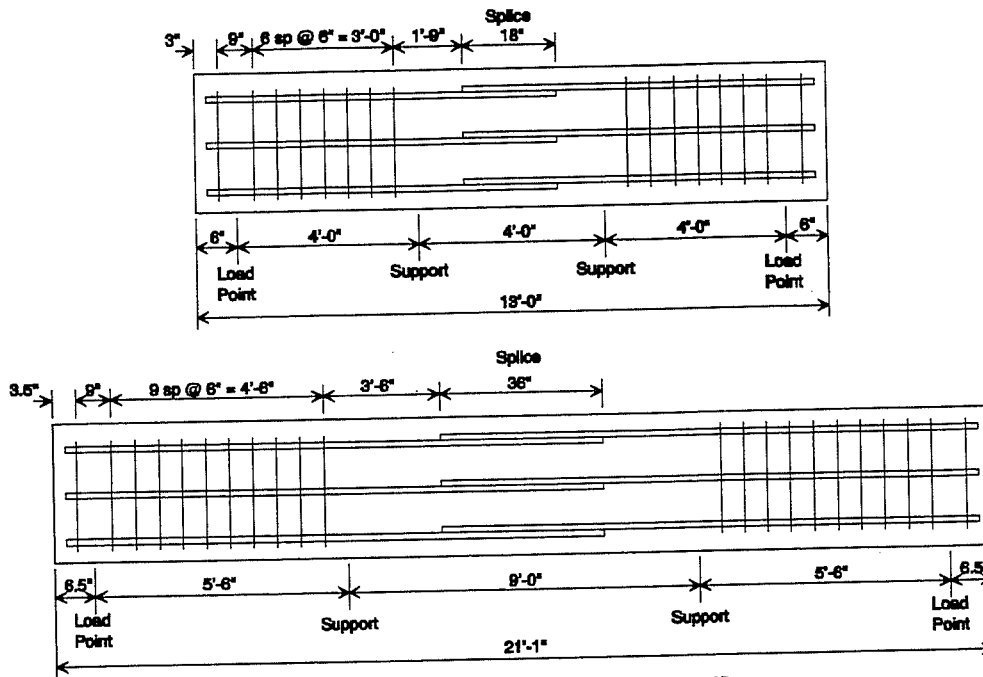
Figure 2.7: Reinforcement Details

Figure 2.8: Splice Support Rod

2.4.3 Casting

All beams in one series were cast together. For the first series, the concrete was cast directly from the ready-mix truck as shown in Figure 2.9. In the second series, the concrete was placed from a bucket that was lifted by an overhead crane as shown in Figure 2.10. Placement with the bucket proved the better method since more control could be achieved over placement locations.

The concrete was placed in two lifts to eliminate segregation. As each lift was being placed, internal vibrators were used to consolidate the concrete. During placement, concrete cylinders were cast. After placement was completed, the beams were screeded.

Once the concrete began to set, lifting hooks were inserted at the support locations, and the beams were finished by trowelling to a fairly smooth finish. The beams were covered with plastic sheeting, and the cylinders were finished in the same manner. For a week after casting, water was sprayed on the concrete to maintain moisture and promote curing.

The forms were stripped after one week. The beams were stacked for storage and curing was discontinued. The cylinders were stripped at the same time as the beams and were cured with the beams.

2.5 Test Setup and Procedure

The testing setup was designed to load down on the beams at the ends producing a constant moment region in the center. The beams were supported by concrete blocks that were grouted to the reaction floor. At the reaction points, rods were placed between two steel plates which distributed the reactions to the concrete and avoided localized crushing. The bottom plates were attached to the concrete base with hydrostone while the upper

Figure 2.10: Casting - Series 2 (Bucket)

Figure 2.9: Casting - Series 1 (Ready-Mix Truck)

plates were seated between the beam and the rod without any grouting. At one support, the rod was welded to the bottom plate to simulate a pin connection while at the other support, the rod was free to simulate a roller.

The load was applied by two 20 ton hydraulic rams at either end of the specimen. A steel reaction beam was placed across the end of the beam with the rams placed on the top flange. The rams reacted against a steel plate that was attached to two tie rods which transferred the load directly to the reaction floor. The loading detail is shown in Figure 2.11.
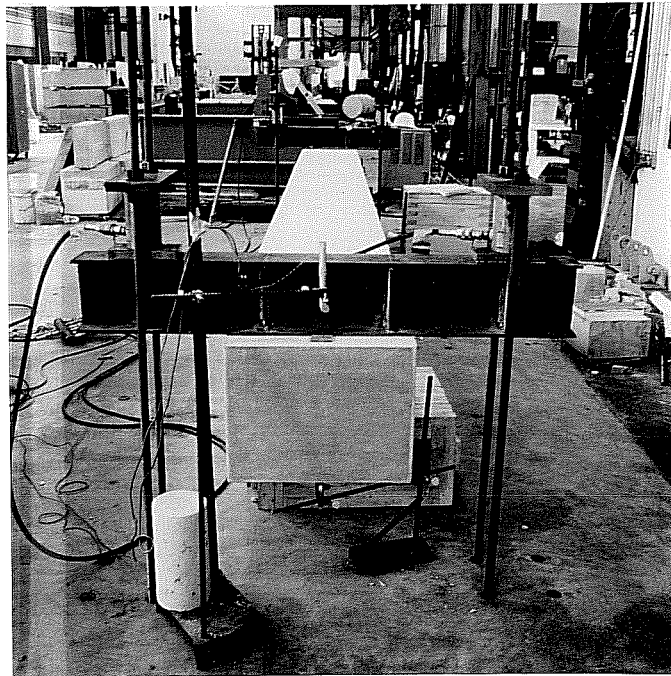
Figure 2.11: Loading Detail

Since two different size beams were being tested, the setup was designed to accommodate both sizes. For the shorter #6 specimens, two concrete blocks as shown in Figure 2.12 were stacked to raise the specimen so that the outer blocks used for the longer #11 specimens would not interfere with the

deflections. These blocks were removed during the #11 tests as shown in Figure 2.13.

The load for all specimens was applied in one kip intervals and was monitored by a 5000 psi pressure transducer. The transducer was connected to a manifold as were hoses to the four rams so that the pressure was the same to each ram. The output from the pressure transducer was read directly on a voltmeter. The loading system was calibrated on a 60 kip universal testing machine.

A 6 inch linear potentiometer was attached at the end of the specimen and connected to an x-y plotter. Along with the output from the pressure transducer, a load versus deflection plot was obtained during testing.

At each load stage, the load was read along with the deflections at the middle of the beam and under the loading point. Deflections were read with 0.001 inch dial gages for Series 1 specimens while a 0.0001 inch digital displacement gage was used for Series 2 specimens. The cracks were marked and crack widths were measured at several locations with a crack comparator. Cracks located between the support and the end of the splice were measured at one specific location along the crack. Cracks were measured at the ends of the lap splices.
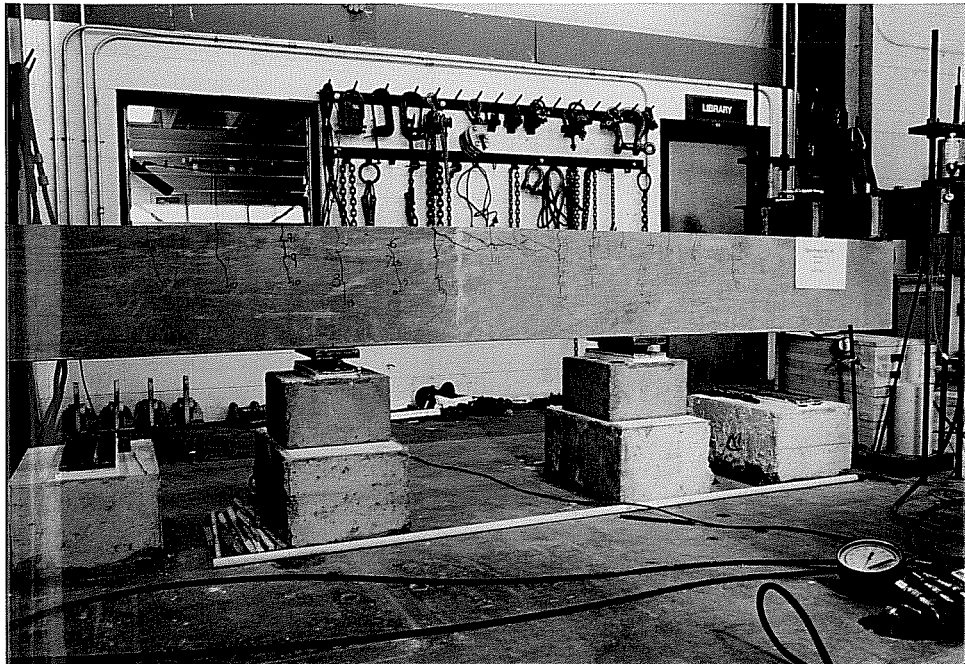
Figure 2.12: #6 Testing Setup
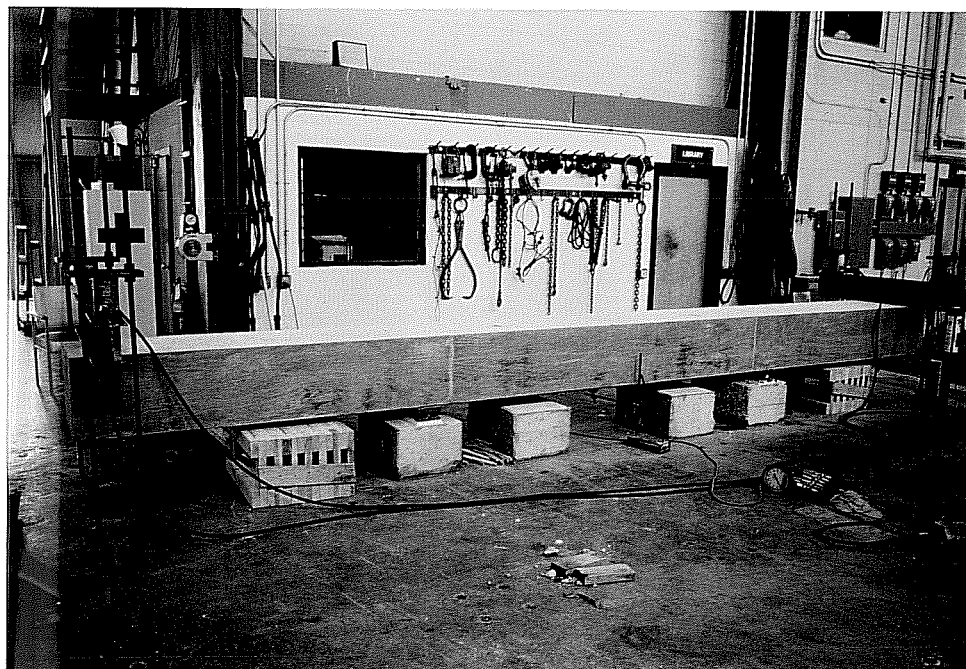
Figure 2.13: #11 Testing Setup

CHAPTER 3

STRUCTURAL BOND - TEST RESULTS

3.1 Introduction

The results of the eight lap splice tests are presented so that comparisons can be made between coated and uncoated bars with respect to beam stiffness, crack widths, and bond strengths. Additionally, the general behavior of specimens during testing is discussed. The overall performance of the coated bars is also compared with epoxy-coated reinforcement.

3.2 General Behavior

3.2.1 Flexural Cracking

Cracking was observed in both coated and uncoated specimens at approximately the same loads. The first cracking usually initiated at the ends of the splice and near the support. As loading increased, cracking was observed in the constant moment region; and existing cracks extended and widened. Of particular note, the cracks over the supports and at the ends of the splice were wider than the rest of the cracks within the constant moment region. Cracks randomly appeared between the splice ends and the supports and within the splice region. Cracks in the splice region did not propagate as far down the beam as the others since there is effectively twice as much steel in this section of the beam.

Flexural cracking was also noted along the shear span. These cracks initiated at the support and continued toward the loading point as loads on the beam increased. The cracking pattern resembled the bending moment diagram. In addition, as the cracks increased in depth, they inclined towards the support to form flexural shear cracks.

3.2.2 Failure

In all tests, the failure was sudden and without much warning which is typical of an unconfined lap splice failure. In a few tests, small longitudinal splitting cracks were evident on the surface over the bars which indicated that failure was near. In most cases, however, only flexural cracks were evident immediately before failure. The extensive spitting cracks shown in Figure 3.1 were visible only after failure. The brittle nature of the failure is evident in Figure 3.2 where cover splitting and the collapse of the beam ends can be seen.

3.2.3 Appearance After Failure

After the test was completed, the cover was removed to inspect the bars and determine exact bar locations. Good adhesion of the concrete to the uncoated bars was noted with concrete being attached to the bar at the deformations (Figure 3.3).

Upon removal of the cover from the coated bars, it was noticed that the bar coating was attached to the concrete cover and very little appeared to be adhering to the bar (Figure 3.4). Several small spots, however, did not adhere to the concrete. The concrete in these spots was discolored; the concrete was darker in color in these locations appearing that the concrete was chemically altered at the coating-concrete interface.
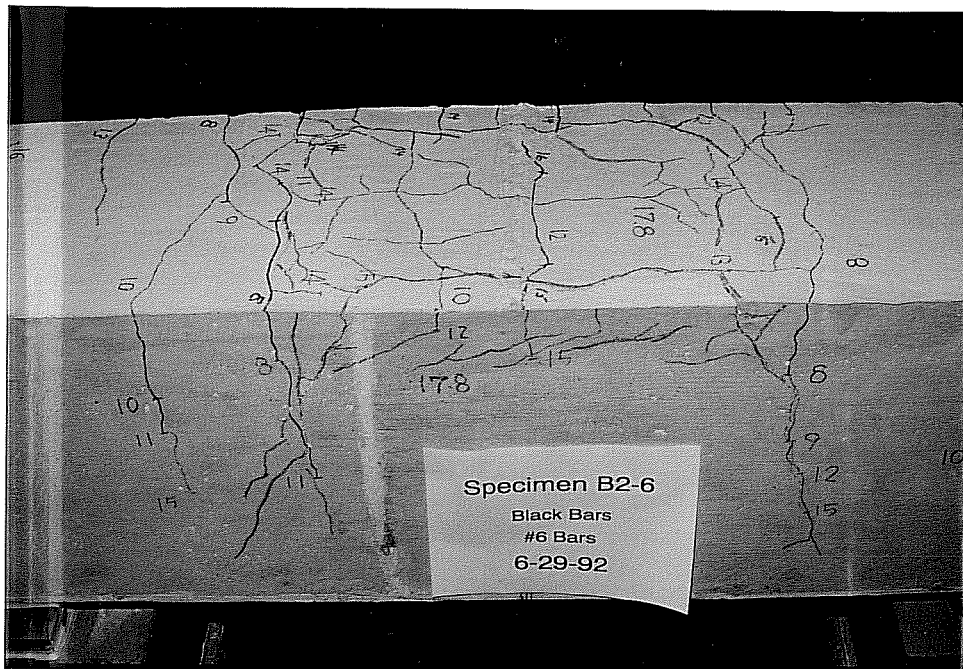
Figure 3.1: Extensive Splitting Cracks
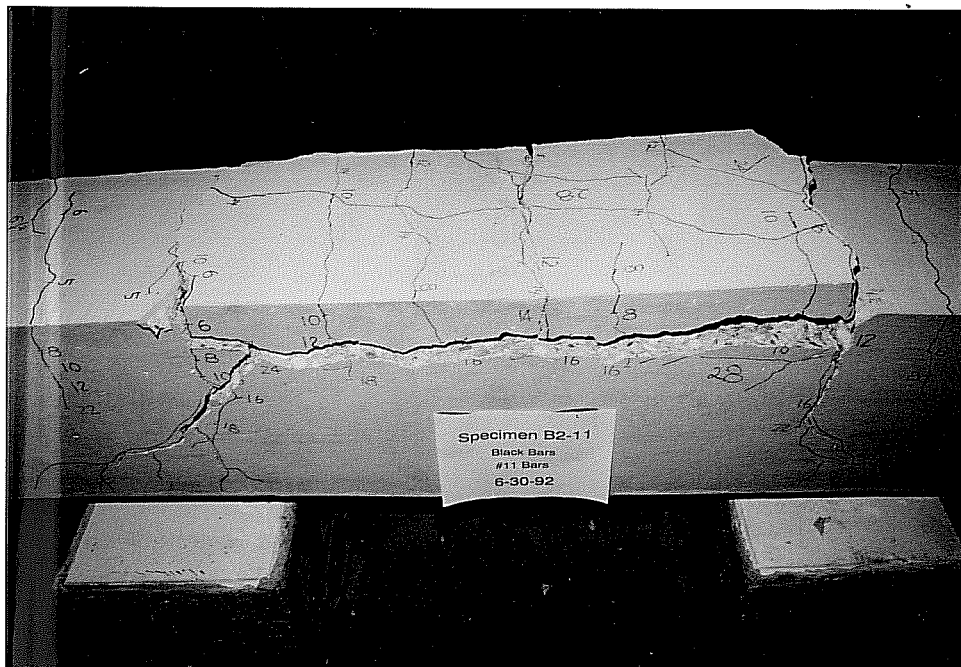
Figure 3.2: Brittle Nature of a Splitting Failure
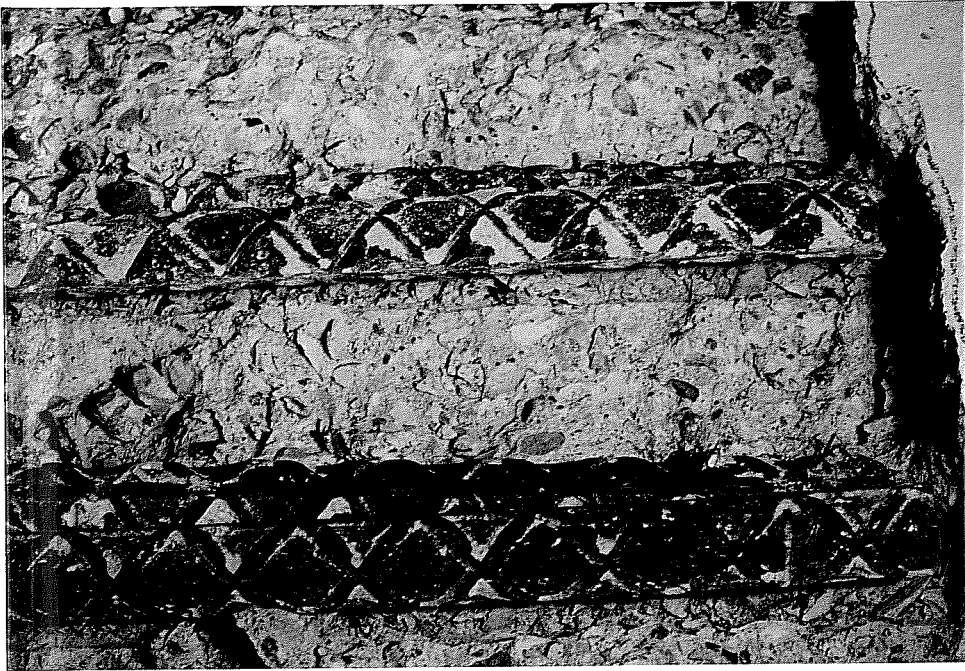
Figure 3.3: Adhesion of Concrete to Uncoated Bars
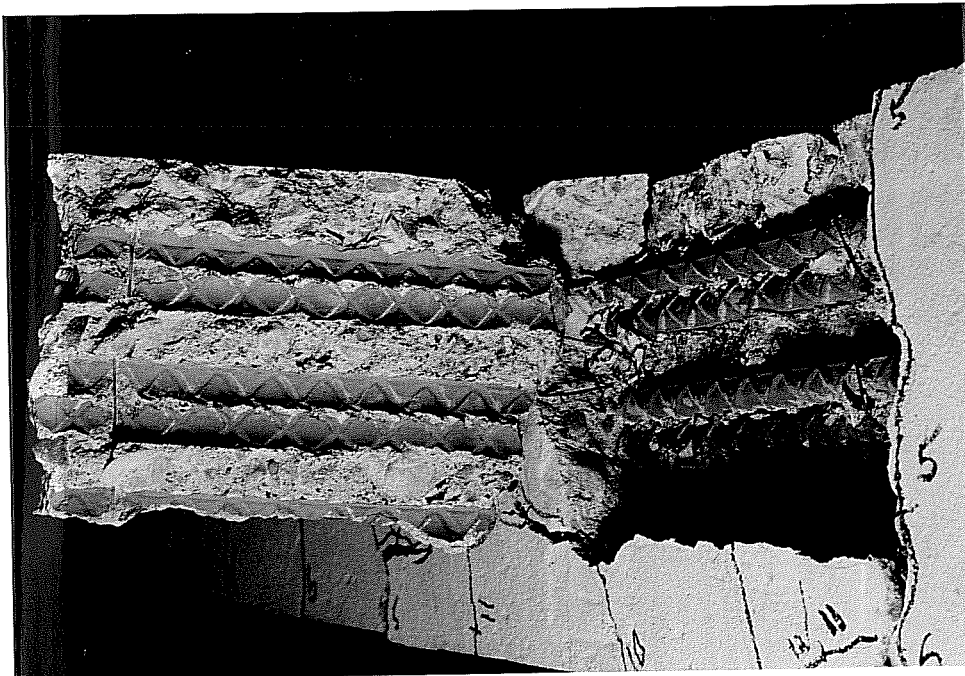
Figure 3.4: Coating Attached to Concrete

3.3 Test Results

The results of the tests are given in Table 3.1. The characteristics of each test specimen are given along with the ultimate load at the ends of the beam and corresponding steel stress. The steel stresses were computed from a cracked section, elastic analysis assuming that concrete carries no tension. Design dimensions of the cross-section were used in all calculations.

Table 3.1: Lap-Splice Test Results						
Specimen	f_c (psi)	l_s (in.)	Cover (in.)	Clear Separation (in.)	P_{max} (kips)	f_{su} (ksi)
B1-6	4730	18	1.5	1.0	15.9	45.7
C1-6	4730	18	1.5	1.0	15.9	45.7
B1-11	4730	36	2.0	4.0	35.7	43.6
C1-11	4730	36	2.0	4.0	37.1	45.3
B2-6	3820	18	1.0	4.0	17.5	47.8
C2-6	3820	18	1.0	4.0	16.5	45.0
B2-11	3820	36	2.0	1.410	27.8	34.8
C2-11	3820	36	2.0	1.410	27.5	34.4

3.4 Beam Stiffness

The stiffness of beams containing coated bars is compared to that of beams containing uncoated bars to determine whether the coating influences the beam stiffness. The comparison is made by plotting end load versus end deflection of a companion set of beams. As evident in Figures 3.5
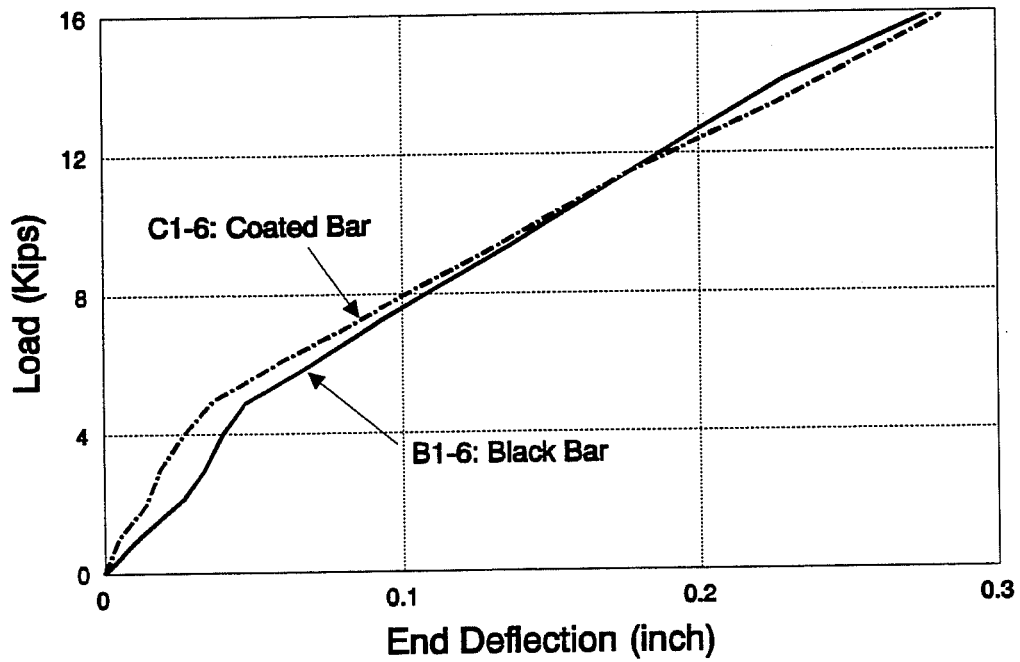
(a) #6 Bars
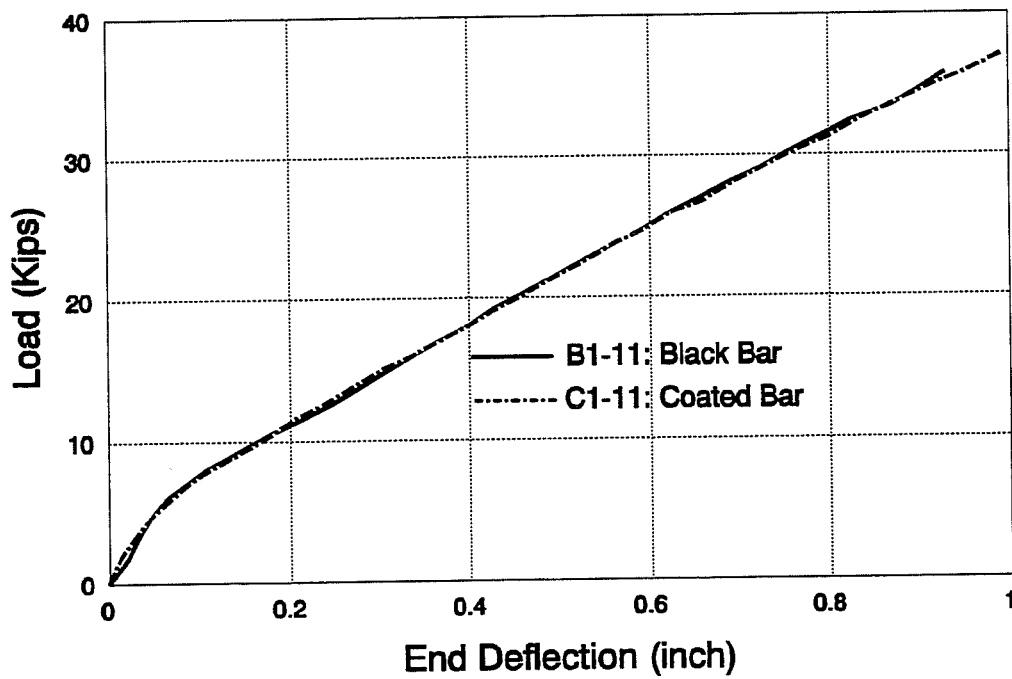
(b) #11 Bars

Figure 3.5: Series 1 Splice Tests
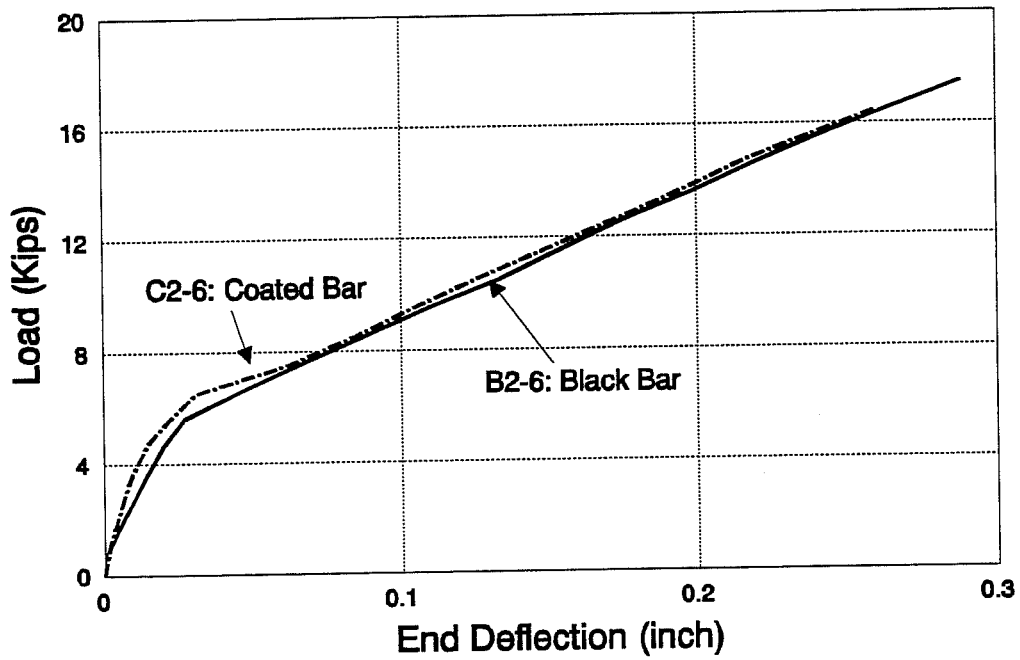
(a) #6 Bars
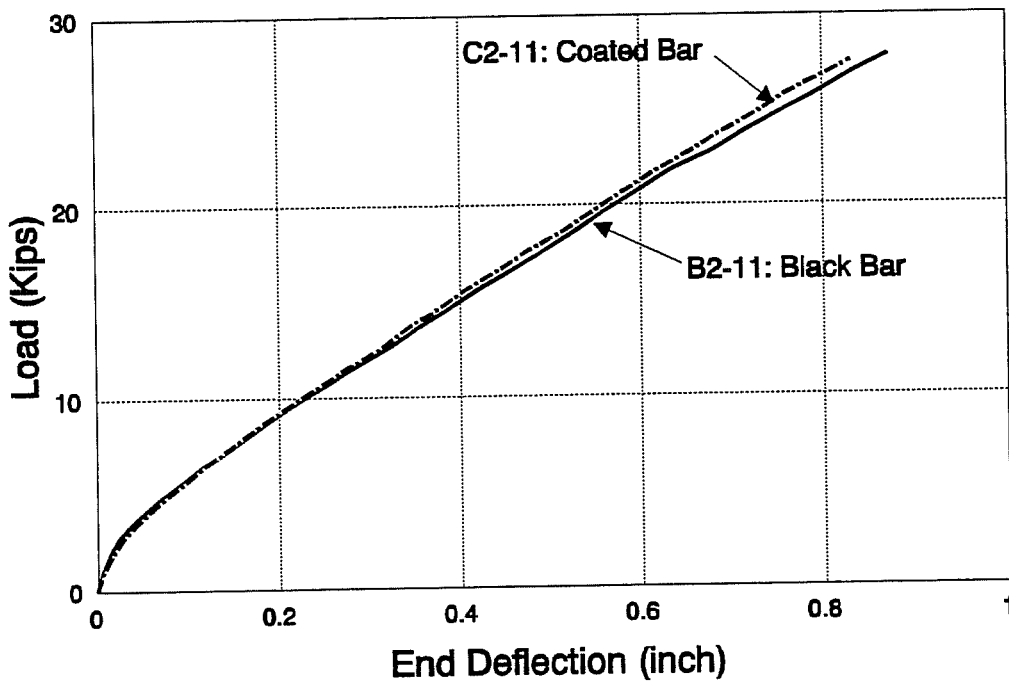
(b) #11 Bars

Figure 3.6: Series 2 Splice Tests

and 3.6, there is virtually no difference between a coated and uncoated bar. In fact, for the #11 tests, the curves are almost exactly the same.

As expected, the cracking load is not influenced since the concrete tensile strength was not affected by reinforcement position or coating. The cracking load is the point where there is an abrupt change in slope as the loading increased.

In summary, the load-deflection characteristics were not affected by the coating.

3.5 Crack Widths

The crack widths of beams containing coated bars are compared with those containing uncoated bars. The comparison is made by plotting steel stresses versus the average crack widths in the constant moment region. As shown in Figures 3.7 and 3.8, only slight differences are evident. In the #11 specimens, it is seen that at higher stresses, the coated bars have a smaller crack width. This may indicate that slightly better bond is achieved with the coated bar than with the uncoated bar. Such an improvement is possible since the coating creates a rough surface on the reinforcing bars. Another fact that seems to indicate better bond is that in the #11 tests, beams with coated bars had several more flexural cracks in the constant moment region. Since the deflections are the same with more cracks, the crack widths must be smaller.

In summary, the cracks widths do not seem to be significantly affected by the coating. The coating may reduce the crack widths which would be beneficial since a smaller crack width reduces the potential for corrosive material to reach the bars.
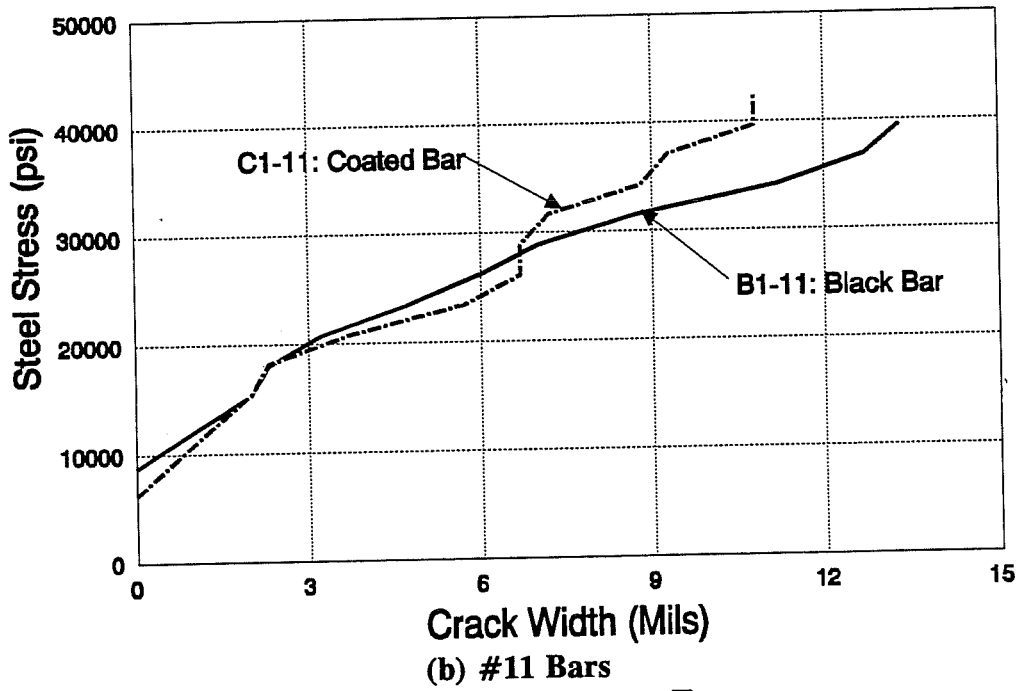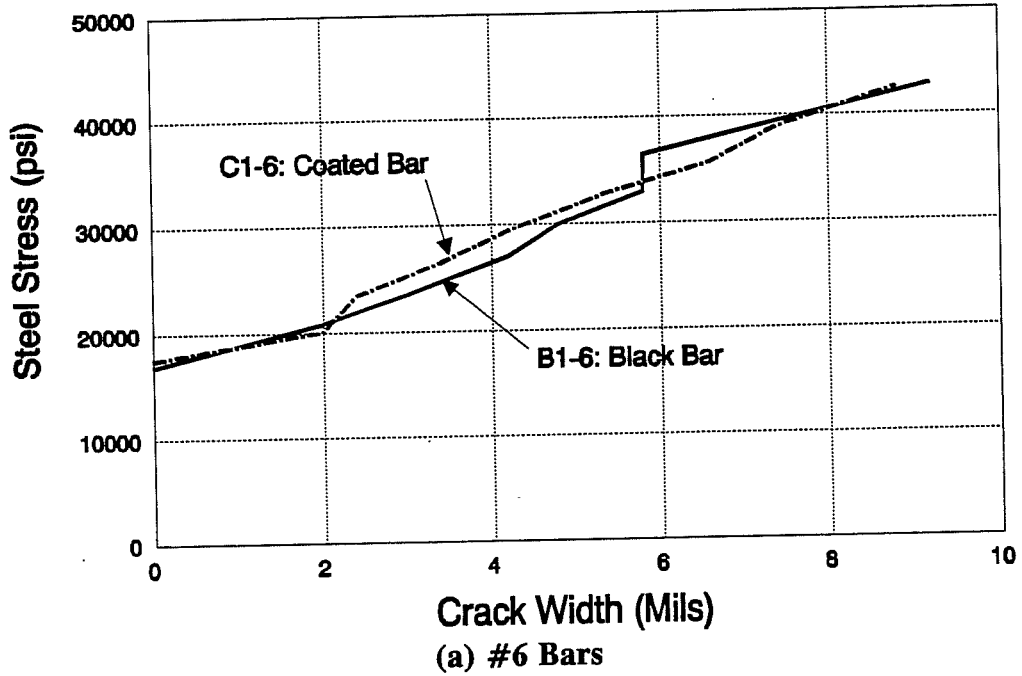
(a) #6 Bars

(b) #11 Bars

Figure 3.7: Series 1 Splice Tests
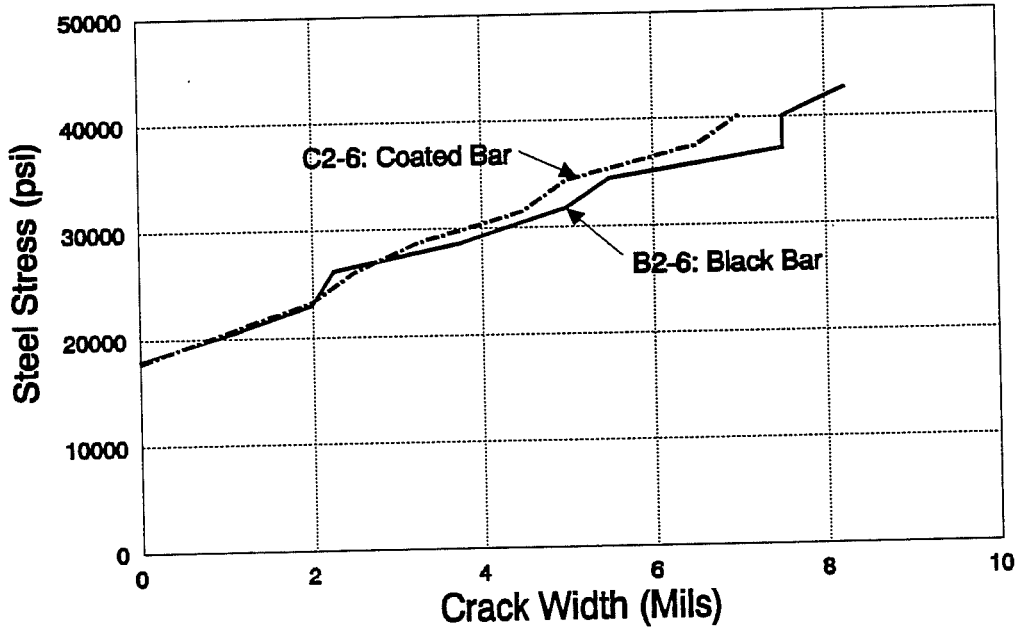
(a) #6 Bars
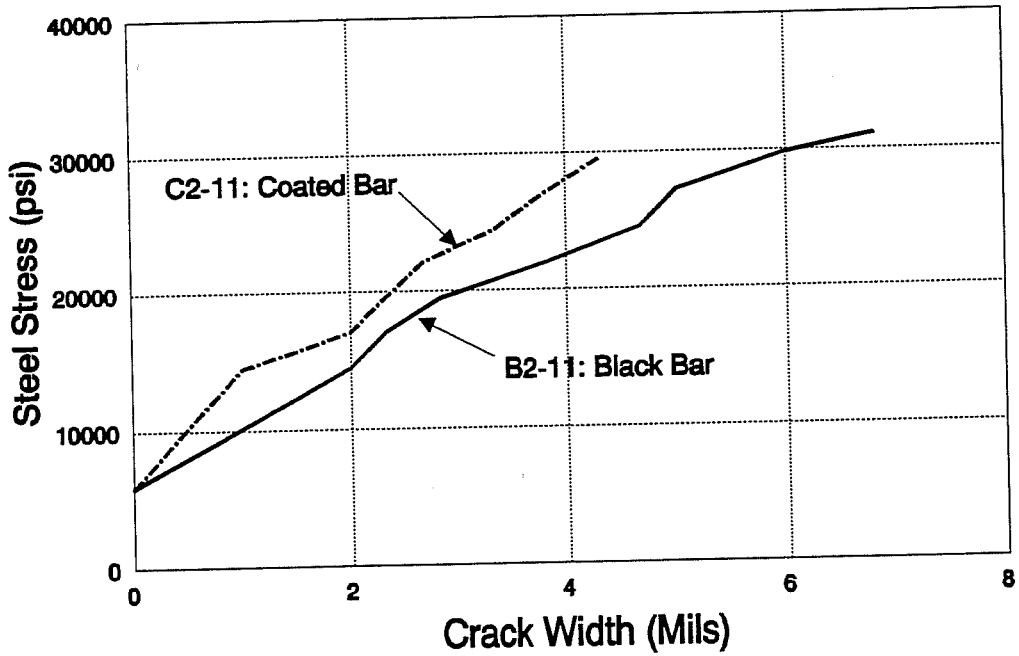
(b) #11 Bars

Figure 3.8: Series 2 Splice Tests

3.6 Bond Strength

The bond strength of each specimen was determined by calculating the average bond stress acting along the splice length. The bond strengths along with the bond ratio of coated to uncoated bars are given in Table 3.2. From a comparison of the bond stresses, it is evident that both coated and uncoated bars reached approximately the same bond strength. The average bond ratio calculated for the coated bars is 0.99 which means that the coating has no effect on the bond strength.

Table 3.2: Lap-Splice Bond Strengths				
Specimen	P_u (k)	f_{su} (ksi)	Bond Strength, u (psi)	Bond Ratio (Coated/ Uncoated)
B1-6	15.9	45.7	474	1.0
C1-6	15.9	45.7	474	
B1-11	35.7	43.6	427	1.04
C1-11	37.1	45.3	443	
B2-6	17.5	47.8	496	0.94
C2-6	16.5	45.0	467	
B2-11	27.8	34.8	340	0.99
C2-11	27.5	34.4	337	

Average Bond Ratio = 0.99

3.7 Comparison of Bond Performance with Epoxy Coated Reinforcement

Epoxy coated reinforcement does not show a significant difference in beam stiffness when compared to ordinary reinforcement as shown in Figure

3.9. This same conclusion was reached for the bars coated with a high ratio zinc silicate. Epoxy coating, however, produces fewer but wider cracks as shown in Figure 3.10. The zinc silicate coating, on the other hand, produced approximately the same number of cracks as ordinary reinforcement with comparable crack widths. Finally, epoxy coated reinforcement significantly lowers the bond strength. The average bond strengths of epoxy coated bars was 0.66 according to Treece[17] in a similar investigation. The high ratio zinc silicate, however, did not affect the bond strength. The average bond strength measured was 0.99.

Bars coated with a high ratio zinc silicate exhibit better bond performance than epoxy-coated reinforcement. The coated bars performed practically the same as ordinary reinforcement and did not show any of the bond related problems experience by the epoxy coated reinforcement.

3.8 Design Recommendations

From the results of the testing performed in this study, it is recommended that current structural provisions governing development lengths for uncoated bars are applicable when designing structural members containing reinforcing steel coated with a high ratio zinc silicate.
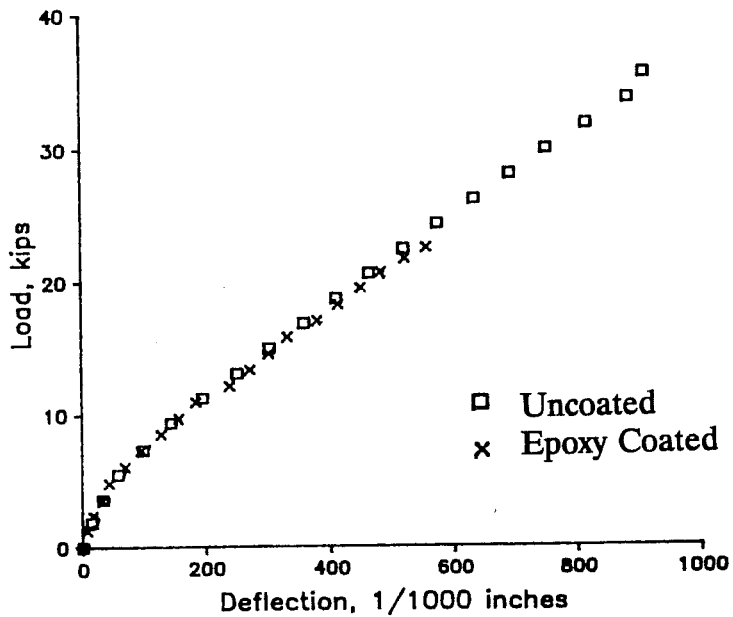
Figure 3.9: Beam End Deflection (Epoxy Coated)[17]
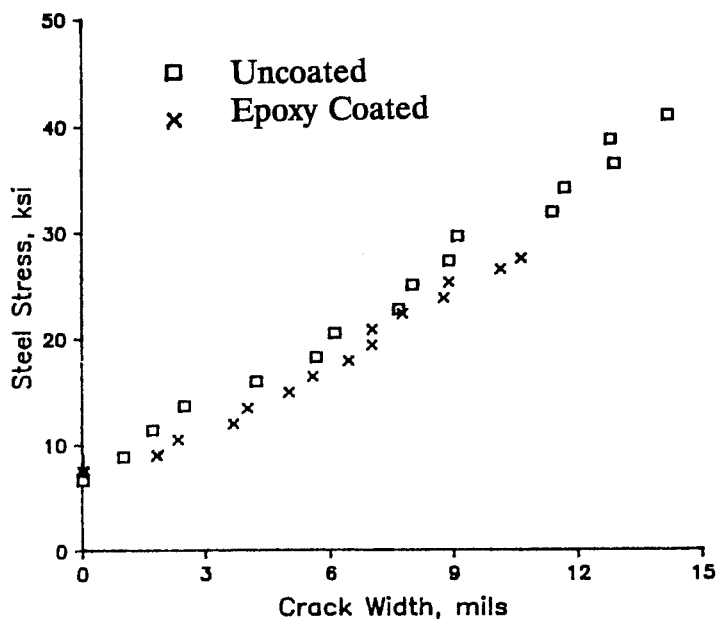
Figure 3.10: Average Crack Widths (Epoxy Coated)[17]

CHAPTER 4

CORROSION - EXPERIMENTAL PROGRAM

4.1 Introduction

Twenty four macrocell specimens were constructed to evaluate the corrosion protection provided by a high ratio zinc silicate. The corrosion current was monitored along with chloride concentration. Additionally, ten air exposure tests were performed for visual observations of accelerated corrosion.

4.2 Design of Specimens

4.2.1 Macrocell Specimens

The macrocell specimens were constructed similar to those used by the FHWA[15] for epoxy-coated bars. The dimensions were exactly the same as macrocell specimens currently under investigation for epoxy-coated reinforcement at the University of Texas at Austin.

The details of the specimens are shown in Figure 4.1. The bottom mat contains three #9 black (uncoated) bars, and the top mat contains one #8 bar which is the bar being tested. The #8 bar was bent to the minimum diameter of bend allowed by ACI 318-89[1] to provide the most severe bending conditions. The specimen dimensions were subsequently based around the bent shape of the bar. The top cover of the specimens is the only variation made regarding specimen dimensions. Two cover dimensions (1 and 2 in.) were used as specimens variables.

Macrocell action is created by setting up a galvanic cell. The corrosion circuit is shown in Figure 4.2. Chloride (NaCl) solution is ponded on top of
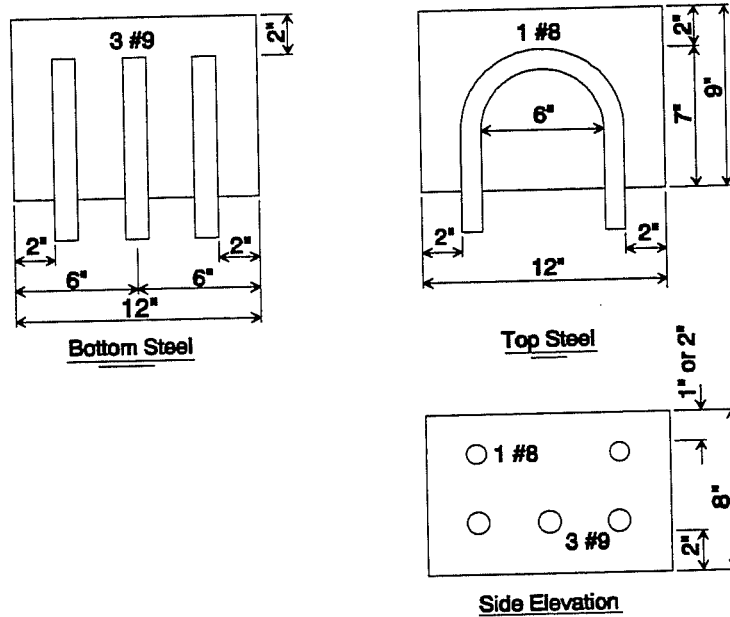
Figure 4.1: Macrocell Details

the specimen which supplies both water and chloride ions for the electrochemical cell. A steel bar is welded to the three bars in the bottom mat for electrical continuity. The circuit is completed by attaching a 100 ohm resistor between the top and bottom mats of reinforcement. The current is determined by measuring the voltage across the resistor which is the potential difference between the top and
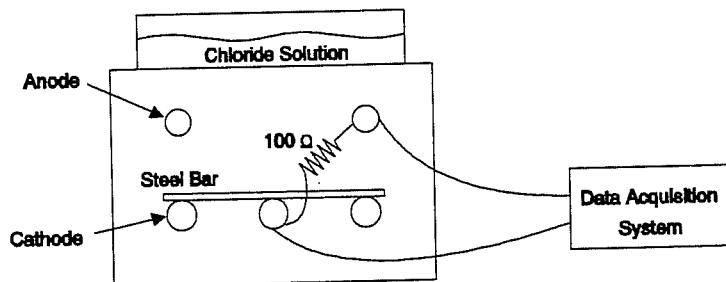
Figure 4.2: Macrocell Circuit

bottom mats. The top mat of steel becomes the anode and the bottom mat becomes the cathode of the galvanic cell.

The chloride content was monitored using nine additional specimens (6 inch concrete cubes) which were exposed to the same NaCl solution. The chloride content was determined by extracting samples from these specimens without disturbing the macrocell tests.

4.2.2 Air Exposure Tests

The air exposure tests are used to complement the macrocell tests. These tests were designed to visually observe the corrosion of reinforcement. Number 8 specimens bent to the same dimensions as the macrocells were placed in buckets of salt solution. Cycling of wet and dry periods accelerates the corrosion process and simulates a splash zone exposure condition without any concrete around the bar.

4.3 Materials

4.3.1 Reinforcing Steel

Both #8 and #9 reinforcing bars were used in the corrosion testing program. The #8 coated bars were obtained from the coating supplier. These bars were grade 60 and had a diamond deformation pattern. The #8 uncoated bars used for control specimens were obtained from a different supplier. They were also grade 60 but had a bamboo deformation pattern.

The #8 bars were bent by a steel fabricator. During bending of the coated bars, the coating severely flaked in the bent region of the bar as shown in Figure 4.3. Little, if any coating remained on the inner and outer radii of the bent bar, but a thin strip of coating remained on the center (neutral axis).

The coating remained intact along the straight portions of the bar outside the bent region except for several damaged areas caused by the steel rollers on the bending machine. The roller damage, however, was concentrated at the transition from the straight to the bent section.

Most of the bars were recoated. The surface of the bars was prepared in two different ways before recoating. Four bars were grit blasted to remove the old coating while the rest of the bars were wire brushed to remove all loose flakes of coating. The bars were subsequently recoated as shown in Figure 4.4. The thickness of the recoating was measured to be approximately 4 mils.

The #9 bars used in the bottom mat of all specimens were grade 60 with a bamboo deformation pattern. These bars were obtained from the same heat of steel so that the cathodes of all specimens would have the same chemical and electrical properties. These properties ensure that the rate of corrosion of the anodes is not influenced by differences in the cathodes.

The #9 bars were prepared for the specimens using a pickling process to provide a clean cathode. The bars were initially grit blasted to a near white finish which removed all mill scale. The bars were subsequently dipped in a 10 percent sulfuric acid solution for 15 minutes. Upon removal, they were rinsed in two baths of clean water for 5 minutes each. Finally, the bars were sprayed with rubbing alcohol to dry the surface.

4.3.2 Concrete

All specimens were cast at the same time with concrete obtained from a ready-mix supplier. A nominal 2500 psi mix with a maximum aggregate size

Figure 4.3: Coating Flaked During Bending
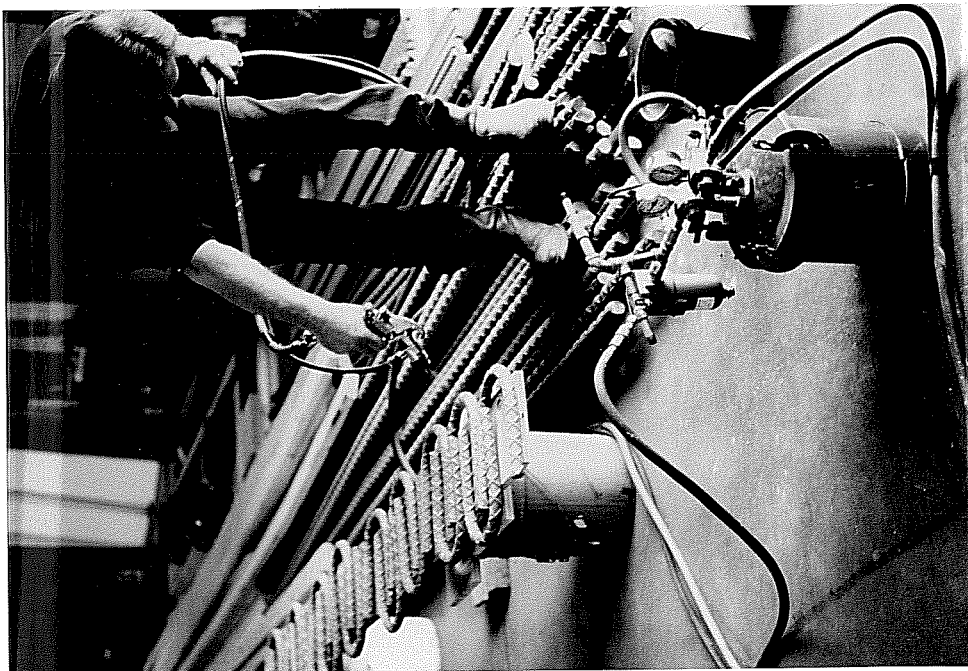
Figure 4.4: Recoating of Bars

of 3/4 inch was used. The mix proportions are given below. All aggregate weights are for saturated surface dry conditions.

Cement (Type I)	373 pcy
Coarse Aggregate	1835 pcy
Fine Aggregate	1414 pcy
Water	200 pcy
Water Reducer-Retarder	16 ozcy

The actual proportions were adjusted according to the moisture content of the aggregates.

The slump was measured before casting at 7 inches. Standard compression tests of three 6 by 12 inch cylinders were used to determine the average compressive strength. The strength-gain curve is shown in Figure 4.5. Additionally, the permeability of the concrete was determined from a 4 by 8 inch cylinder using the standard test for Rapid Determination of the Chloride
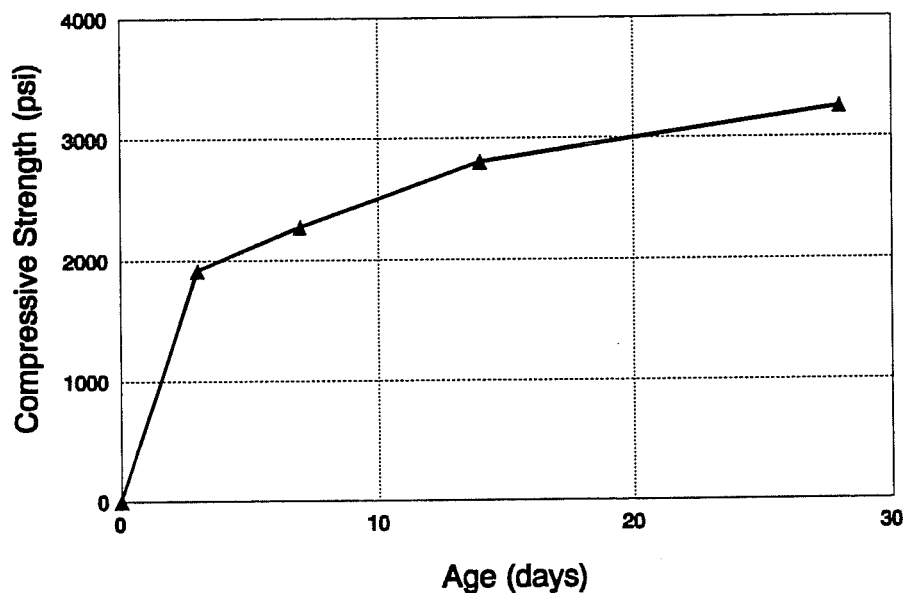
Figure 4.5: Macrocell Concrete Strength Gain

Permeability of Concrete (AASHTO T277-83). The permeability was 15700 coulombs which indicates a very high permeability.

4.4 Specimen Variables

The difficulties encountered during the bending of the bars dictated the variables which were considered. The macrocell specimens tested within this study along with the variations are given in Table 4.1. The notation used to identify each specimen consists of a letter followed by a number. The letter identifies the bar conditions as listed in the table while the number that follows indicates the top cover dimension. Specimen replicates are further identified by a replicate number which follows the specimen identification. As an example, C1-2 indicates the second replicate of a coated bar with a 1 inch top cover.

The details of the different bar conditions are presented below. Black describes uncoated bar specimens that are used as control specimens. These bars are used to determine the corrosion current that exists without corrosion protection measures.

Coated describes coated bars that were machine bent. It was uncertain if the small amount of coating that remained on the bar after bending is sufficient for corrosion protection. Therefore, this condition was selected as a variable to determine if recoating is necessary and if a severely damaged coating can still provide corrosion protection.

Recoated describes coated bars that were bent and subsequently recoated. The surface for these bars was prepared by wire brushing to remove loose flakes of coating. This surface preparation represent a possible method

fabricators could use to recoat fabrication damage. In addition, the bar condition represents the best possible protection with no coating damage.

Table 4.1: Macrocell Specimens			
Specimen	Bar Condition	Top Cover (in)	Number of Specimens
B1	Black	1	2
B2	Black	2	2
C1	Coated	1	3
C2	Coated	2	3
R1	Recoated	1	3
R2	Recoated	2	3
D1	Damaged	1	3
D2	Damaged	2	3
G1	Grit Blasted	1	1
G2	Grit Blasted	2	1

Damaged describes bars that are the same as used for the recoated condition with the exception that coating damage was induced. The recoated bars would be an ideal condition which does not necessarily represent the condition that would exist under field conditions. Damage is normally introduced due to transportation, handling, and placement. In addition, damage can also be introduced by vibrators during casting. The coating was damaged by dropping and rubbing two bars together in order to simulate possible field conditions.

Finally, grit blasted describes coated bars that were bent and subsequently recoated. The surface of these bars, however, was prepared for recoating by grit blasting the flaked coating. Only one specimen of each top cover was used since these are similar to the recoated condition. In addition, this method of surface preparation does not seem as likely to be used by fabricators.

The air exposure tests use the same labels for bar conditions. The variables studied during these tests are shown in Table 4.2. These specimens are identified by the letter of the bar condition followed by the replicate number. For example C-2 indicated the second replicate of a coated bar.

Table 4.2: Air Exposure Specimens		
Specimen	**Bar Condition**	**Number of Specimens**
B	Black	3
C	Coated	3
R	Recoated	1
D	Damaged	2
G	Grit Blasted	2

4.5 Construction of Specimens

4.5.1 Formwork

The formwork for the macrocell specimens consisted of a plywood base with plywood dividers that formed 24 individual boxes as shown in Figure 4.6.

The front plywood panel was predrilled to position the steel at the proper dimensions.
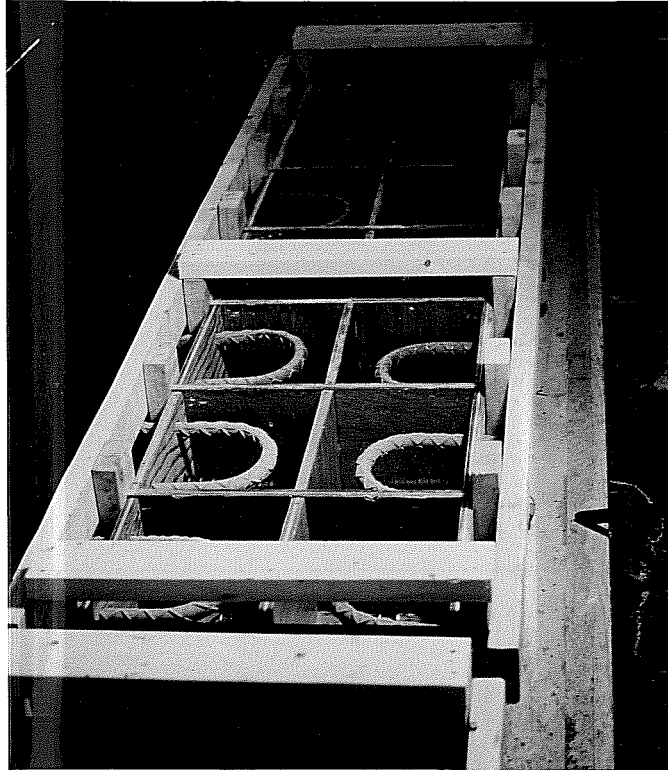
Figure 4.6: Formwork

The formwork was completed by placing wales along the top of both sides of the forms and several braces across the forms which were used to maintain the proper dimensions of specimens during casting.

The formwork for the companion chloride specimens was similarly constructed. These specimens, however, did not require braces since they were fairly small and the overall dimensions were not critical.

4.5.2 Placement of Steel

The reinforcement was prepared for the formwork as described previously. The steel was placed into the formwork by inserting the bars through the front plywood panel as shown in Figure 4.7. The bottom bars were supported by 2 inch steel chairs and the top bar was held in position by wire attached to the bar on the outside of the forms. The wire was tensioned in order to hold the bar at the proper dimensions.

4.5.3 Casting

All specimens were cast as shown in Figure 4.8. The concrete was placed in one lift and consolidated using internal vibrators inserted only at the back sides of specimens to ensure that the steel was not shifted or damaged. During placement, chloride penetration specimens and cylinders were also cast. The specimens were screeded immediately after casting and trowelled shortly after. Plastic sheeting was placed to maintain the moisture. All forms and cylinder molds were removed at the same time approximately four weeks after casting.

4.6 Test Setup and Procedure
4.6.1 Macrocell Tests

The macrocell specimens were coated with a concrete water seal along the four side surfaces to simulate an infinite slab where concrete extends in all directions. A plastic dike was attached with silicone to the top surface of the specimens to contain the chloride solution. A steel bar was welded to the three #9 bars of the bottom mat, and clamps were attached to the top and bottom reinforcement. The corrosion circuit was completed by connecting the
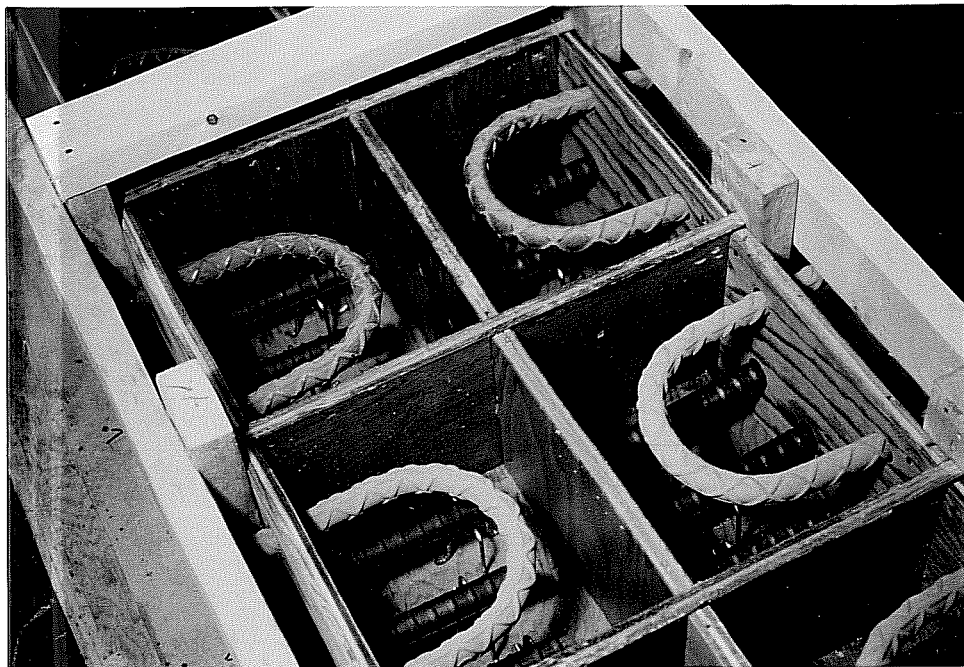
Figure 4.7: Steel Placement

Figure 4.8: Casting

wires as shown in Figure 4.9. Finally, oil was applied to the exposed bars to prevent corrosion outside of the specimen.
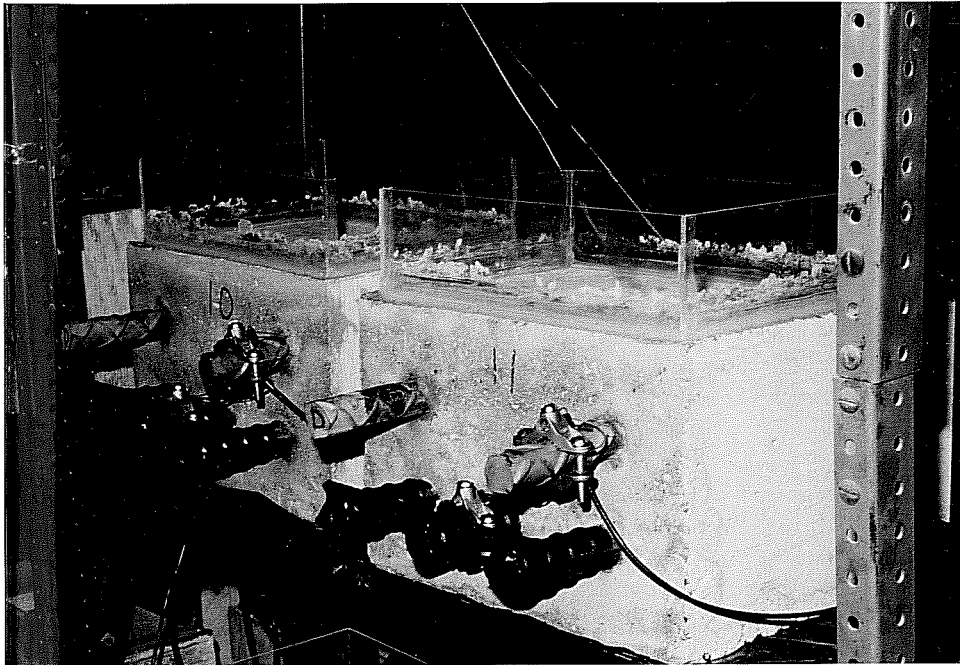
Figure 4.9: Completed Macrocell Specimens

The macrocell tests were maintained in a four week cycle. They were ponded with a 3.5 percent salt solution for a two week period after which the solution was removed and a drying period started. After two weeks, the cycle was repeated. Evaporation of the solution was controlled by covering the dikes with plywood, and voltage readings were taken every week by a data acquisition system.

The chloride penetration specimens were constructed the same as the macrocell specimens and maintained in the same four week cycle. Samples were tested periodically to determine the chloride penetration. Multiple holes

were drilled at various depths and the concrete powder was collected. The powder was then analyzed using a standard procedure for chloride concentration in concrete.

4.6.2 Examination of Bar After Concrete Removal (Autopsy)

After approximately seven months of exposure, selected macrocell specimens were removed from testing to examine the rebar for signs of corrosion. One chloride sample was taken at various depths from each specimen to determine the variation of chloride concentration and determine the chloride concentrations at the level of the steel. The specimens were carefully cut open to avoid disturbing the reinforcement and any possible corrosion products. Saw cuts were made around the perimeter (three sides) of the specimen slightly under the level of the bar. Additional cuts were made on the top surface along the bar. The cuts enabled three chunks of concrete to be removed with a pry-bar which exposed the bar. Finally the bar could be lifted out of the specimen by tapping the protruding legs of the bar with a hammer.

4.6.3 Air Exposure Tests

The air exposure tests were maintained in a one week cycle. The specimens are shown in Figure 4.10. The bars were dipped in buckets containing a 3.5 percent salt solution for 4 days. The specimens were then removed for 3 days of air drying to complete the cycle. Visual observations were made periodically to monitor the corrosion.

Figure 4.10: Air Exposure Specimens

CHAPTER 5

CORROSION - TEST RESULTS

5.1 Introduction

The results of twenty four macrocell tests are presented to evaluate the performance of rebar coated with a high ratio zinc silicate. Results presented include electrical current measurements and an autopsy report of the bar specimen after removal from the concrete. In addition, the results of air exposure tests are used to complement the macrocell tests and contrast the different exposure environments.

5.2 Test Results and Autopsy Reports

The results of the macrocell tests were recorded by plotting the electrical current versus the time of exposure. In addition an autopsy of the selected specimens was performed. The results of these investigations are broken down into the appropriate bar condition categories and concrete cover dimensions.

5.2.1 Black

The results of the control tests are plotted in Figure 5.1. The currents displayed are directly related to corrosion of steel. It is evident from these currents that the onset of corrosion is delayed by the additional one inch of concrete cover.

An autopsy of the rebar was not performed since it is evident that the current readings represent significant corrosion of the steel. Severe corrosion has been experienced by all air exposure specimens.

50
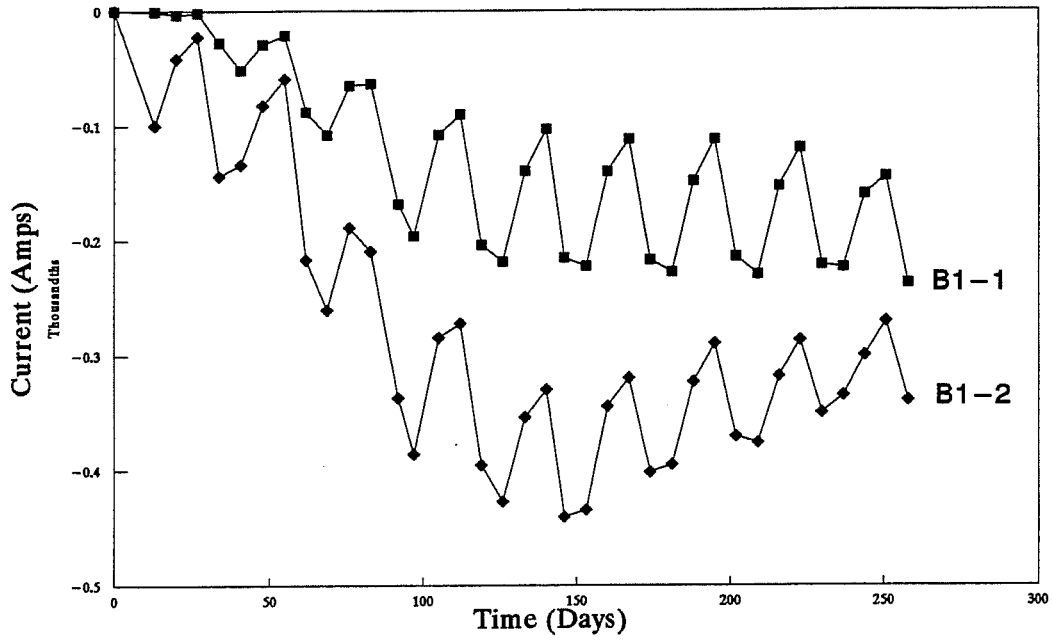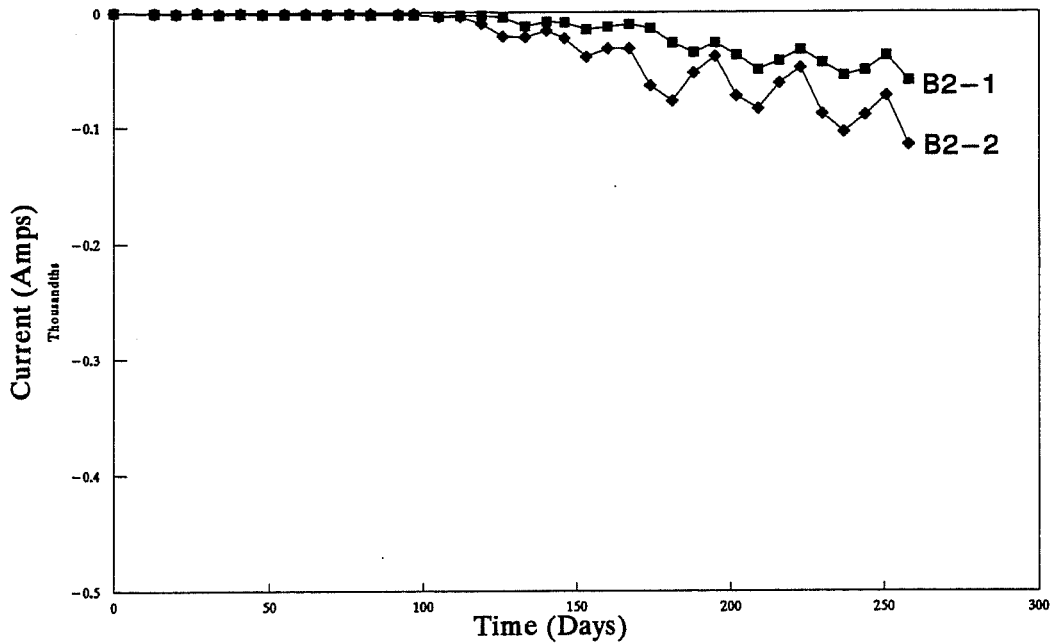
(a) 1 inch Cover

(b) 2 inch Cover
Figure 5.1: Macrocell Tests - Black Bars

5.2.2 Coated

The results of the coated bar tests are shown in Figure 5.2. By comparing the results with the control specimens it appears that the coating slightly delayed the onset of corrosion. The current, however, increased very rapidly once corrosion began, reaching if not exceeding the currents of the control specimens. It is not possible to distinguish whether the current was caused by zinc corrosion (sacrificial action) or steel corrosion. An autopsy was performed on Specimens C1-2 and C2-3 to determine the type and extent of corrosion occurring on the bar. The specimens were opened after 209 and 237 days of exposure respectively.

Specimen C1-2 (Figure 5.3) showed corrosion over an extensive area of the bar extending from the beginning of the bend for several inches into the bent region of the bar. The corroded area was on the resistor side of the bar and extended on both the top and bottom. The most severe corrosion occurred on the bottom surface as shown. A blackish corrosion product was present immediately after removing the concrete which changed to a reddish-brown color after exposure to air. Several days after the bar was removed, small spots of rust were evident in the entire bent region of the bar. The corrosion was not intense, but was apparent as small specks in the region where the coating flaked due to fabrication. Upon removal of the corrosion product from the severely corroded region, pitting was also noted. The chloride content at the level of the steel was found to be 0.20 percent by weight of concrete.

Specimen C2-3 was selected for study since corrosion activity was evident for only 35 days according to the current measurements. This specimen, therefore, would indicate if the current indicated cathodic protection or
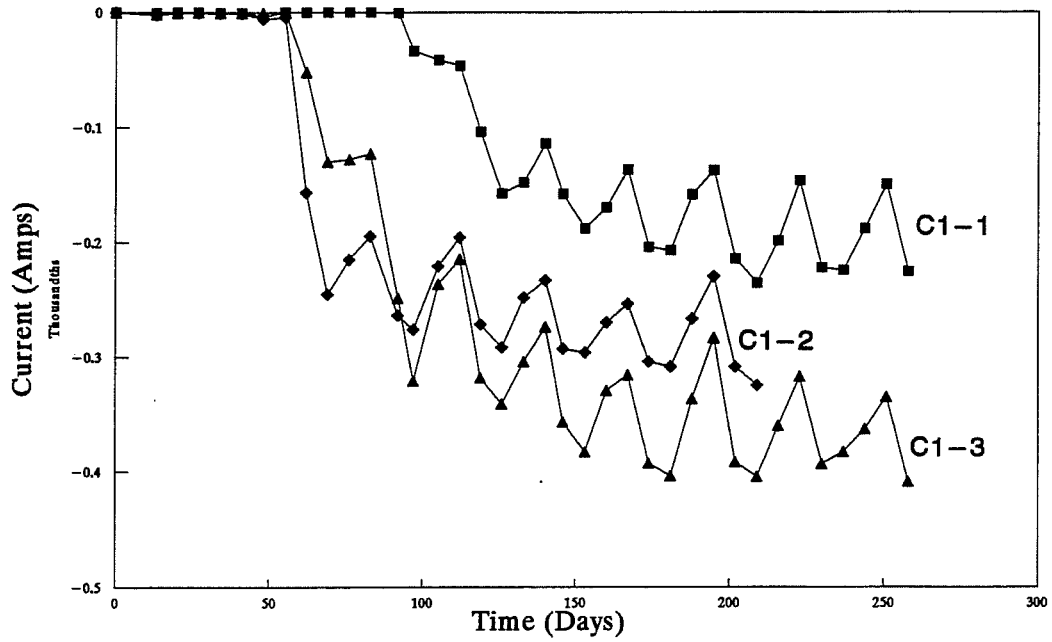
(a) 1 inch Cover
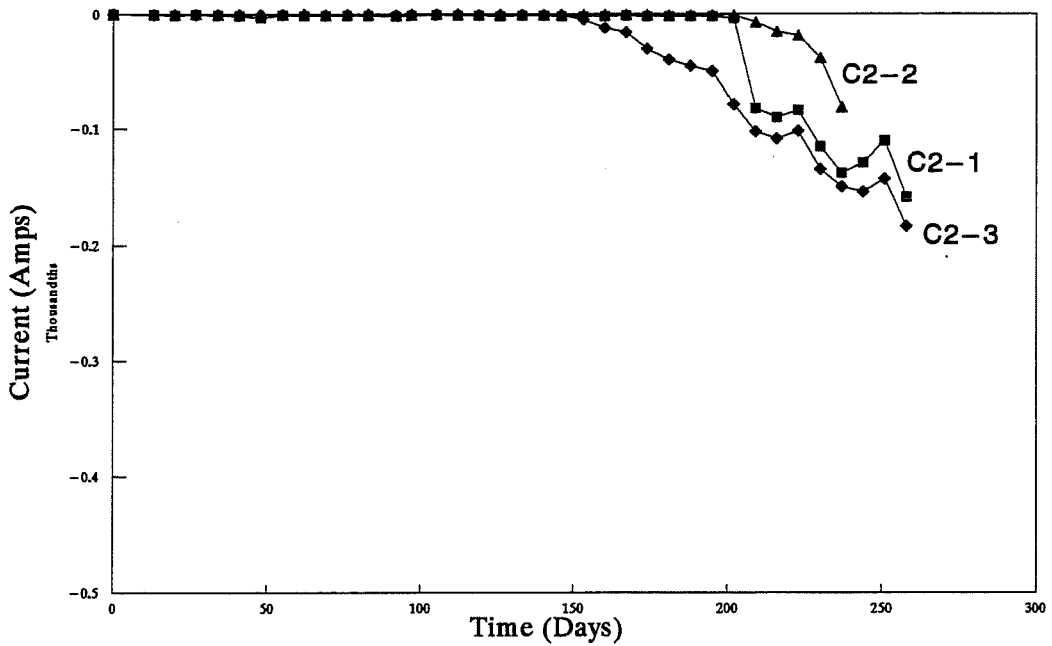
(b) 2 inch Cover
Figure 5.2: Macrocell Tests - Coated Bars

Figure 5.3: Specimen C1-2

Figure 5.4: Specimen C2-3

corrosion of steel. The bar had corrosion on the top from the neutral axis to the outside diameter of the bend as shown in Figure 5.4. The relatively small spot appeared in the middle of the bent region. The corrosion product was blackish and turned reddish-brown after air exposure. No corrosion was found along the entire bent region due to flaked coating as was found with Specimen C1-2. The chloride content at the level of the steel was found to be 0.04 percent by weight of concrete.

Severe corrosion occurred on all air exposure specimens in the bent region of the bar as shown in Figure 5.5.
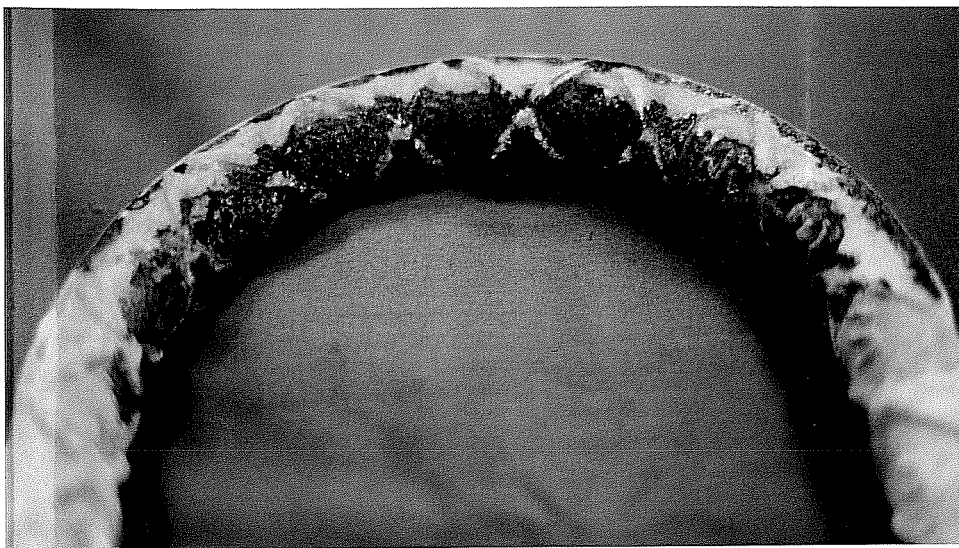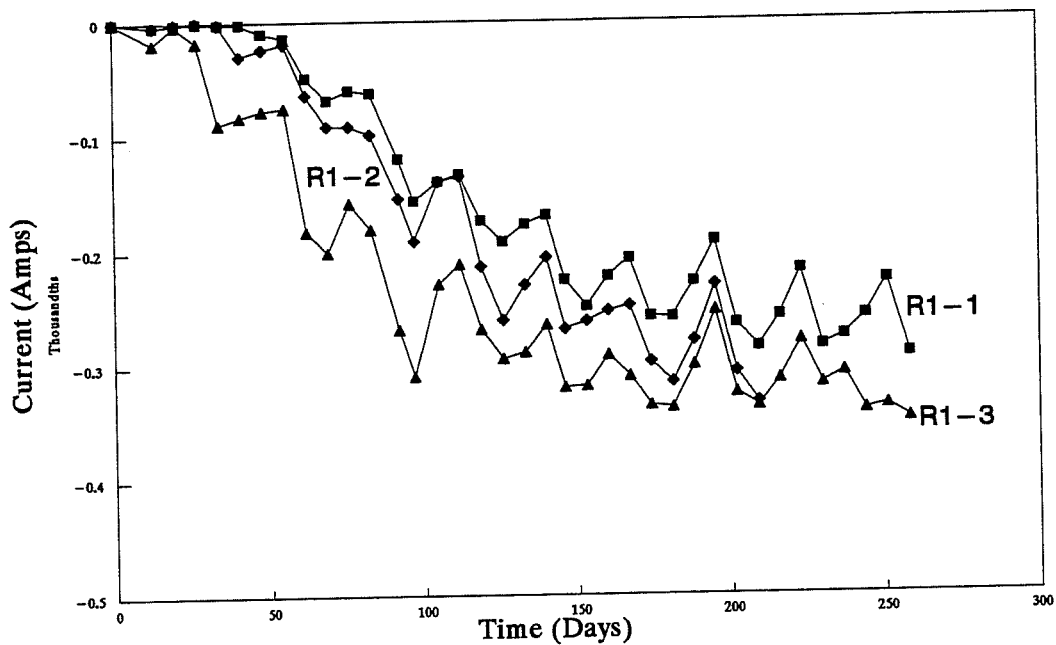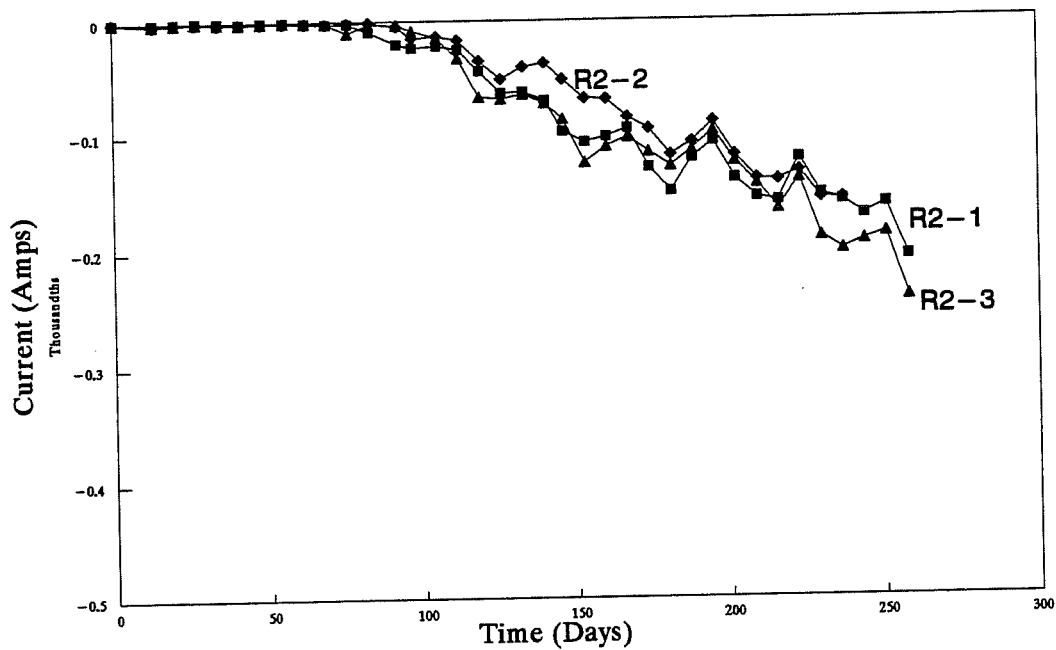

Figure 5.5: Air Exposure Tests - Coated Bar

5.2.3 Recoated

The results of the recoated bar tests are presented in Figure 5.6. By comparing the results with the control specimens, it is apparent that the coating did not affect the time to corrosion. An autopsy was performed on

(a) 1 inch Cover

(b) 2 inch Cover
Figure 5.6: Macrocell Tests - Recoated Bars

Specimens R1-2 and R2-2 which were opened after 209 and 237 days of exposure respectively.

Specimen R1-2 showed extensive corrosion on the middle of the outside diameter of the bend as shown in Figure 5.7. Corrosion was also evident on the inside diameter of the bend but was not as intense. The corrosion product was blackish upon removal of the bar and converted to reddish-brown with exposure to air. The chloride content at the level of the steel was found to be 0.29 percent by weight of concrete.

Specimen R2-2 (Figure 5.8) also showed extensive corrosion on the middle region of the outside diameter of the bend. The corrosion was spread over a larger area than R1-2, but was not as intense. The corrosion product appeared blackish and blackish-grey in less attacked spots. A reddish-brown product was evident in small spots upon removal and was seen over most of the corroded area after exposure to air. The chloride content at the level of the steel was found to be 0.16 percent by weight of concrete.

No corrosion damage has been observed on the air exposure specimens as shown in Figure 5.9.

5.2.4 Damaged

The results of the damaged bar tests are presented in Figure 5.10. The results are similar to those of the recoated bars. An autopsy was performed on Specimens D1-2 and D2-1 which were opened after 209 and 237 days of exposure respectively.

Specimen D1-2 (Figure 5.11) showed severe corrosion on the inside diameter of the bend on the resistor side. In addition, another corrosion site was located at the middle of the inside diameter of the bend. The corrosion

Figure 5.7: Specimen R1-2

Figure 5.8: Specimen R2-2

Figure 5.9: Air Exposure Tests - Recoated Bar

product was initially blackish and turned reddish-brown after exposure to air. Upon removal of the corrosion products, pitting of the steel was evident in the region. The chloride content at the level of the steel was found to be 0.28 percent by weight of concrete.

Specimen D2-1 had three different corrosion sites all on the resistor side of the bar that are shown in Figure 5.12. One small corrosion spot was evident at the beginning of the bend. Another small spot was located on the middle of the outside diameter of the bend. The most severe corrosion was found in between these locations. Corrosion was evident on both the inside and outside diameters of the bend in this location. The corrosion product was blackish in all locations and converted to reddish-brown after air exposure.
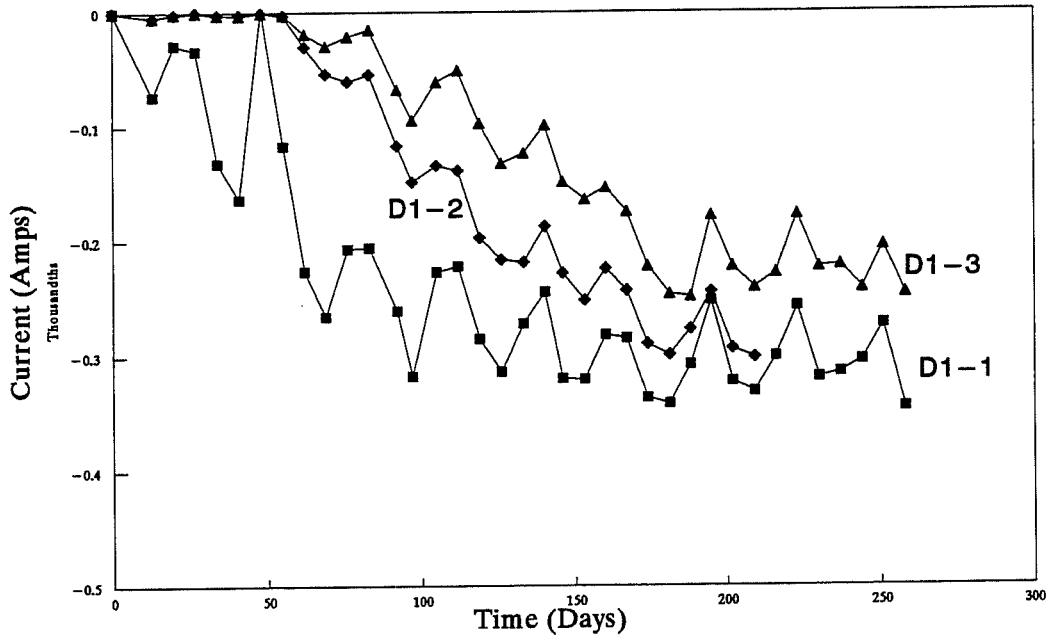
(a) 1 inch Cover
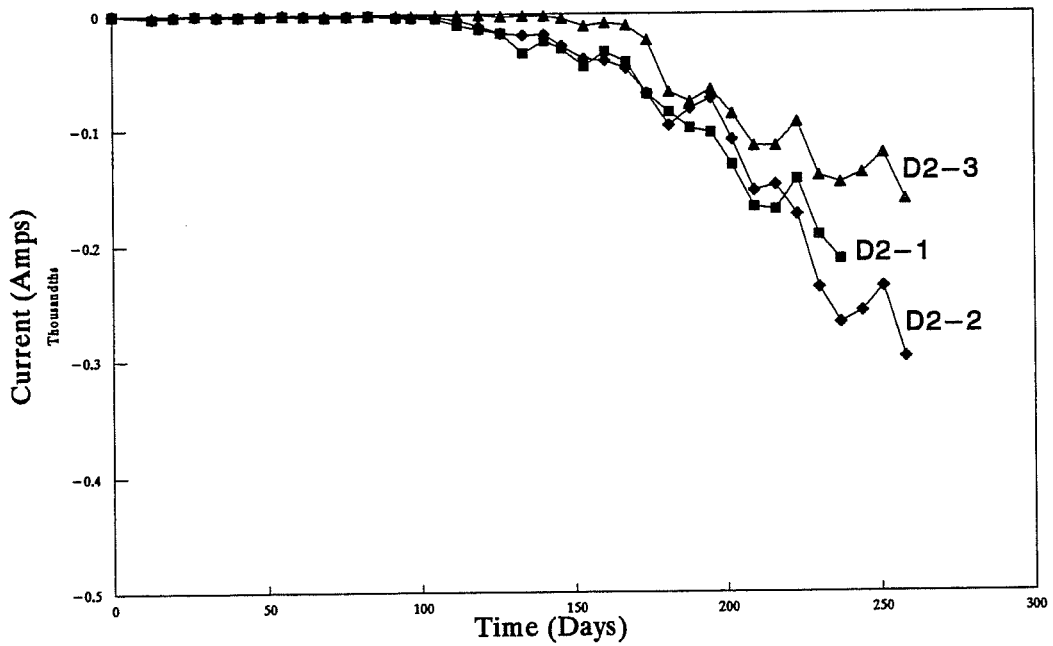
(b) 2 inch Cover

Figure 5.10: Macrocell Tests - Damaged Bars

Figure 5.11: Specimen D1-2

Figure 5.12: Specimen D2-1

The small spot on the middle of the bar was reddish in color upon opening of the specimen. The chloride content at the level of the steel was found to be 0.14 percent by weight of concrete.

No corrosion damage has been experienced by the air exposure specimens.

5.2.5 Grit Blasted

The results of the grit blasted bar tests are presented in Figure 5.13. The results are compared with the recoated tests since these bars had a similar coating condition (no coating damage). Upon comparison, it is obvious that there is essentially no difference in the results. An autopsy was performed on Specimens G1-1 and G2-1 which were both opened after 216 days of exposure.

Specimen G1-1 showed severe corrosion on the bottom in the middle of the bent region as shown in Figure 5.14. Further corrosion was evident on the top of the bar from the middle of the bar continuing for several inches on the resistor side of the bend. The corrosion product was blackish upon opening the specimen and converted to reddish-brown after air exposure. The chloride content at the level of the steel was found to be 0.36 percent by weight of concrete.

Specimen G2-1 (Figure 5.15) showed corrosion only in one 3/4 inch spot on the outside diameter in the middle of the bend. The corrosion product was black and converted to reddish-brown after air exposure. The chloride content at the level of the steel was found to be 0.09 percent by weight of concrete.

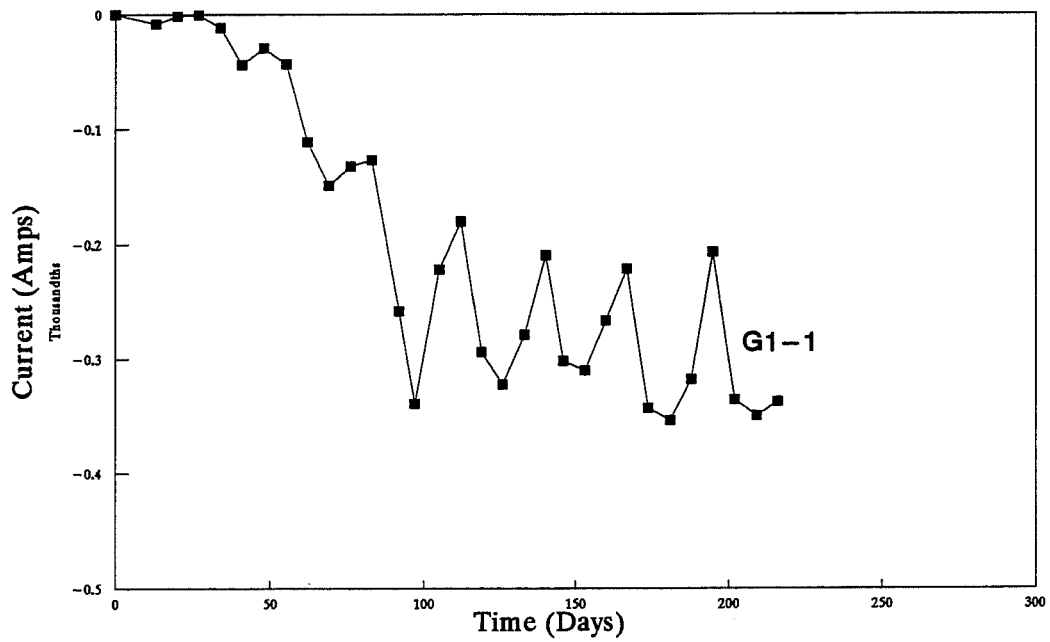No corrosion damage has been experienced by the air exposure specimens.

(a) 1 inch Cover
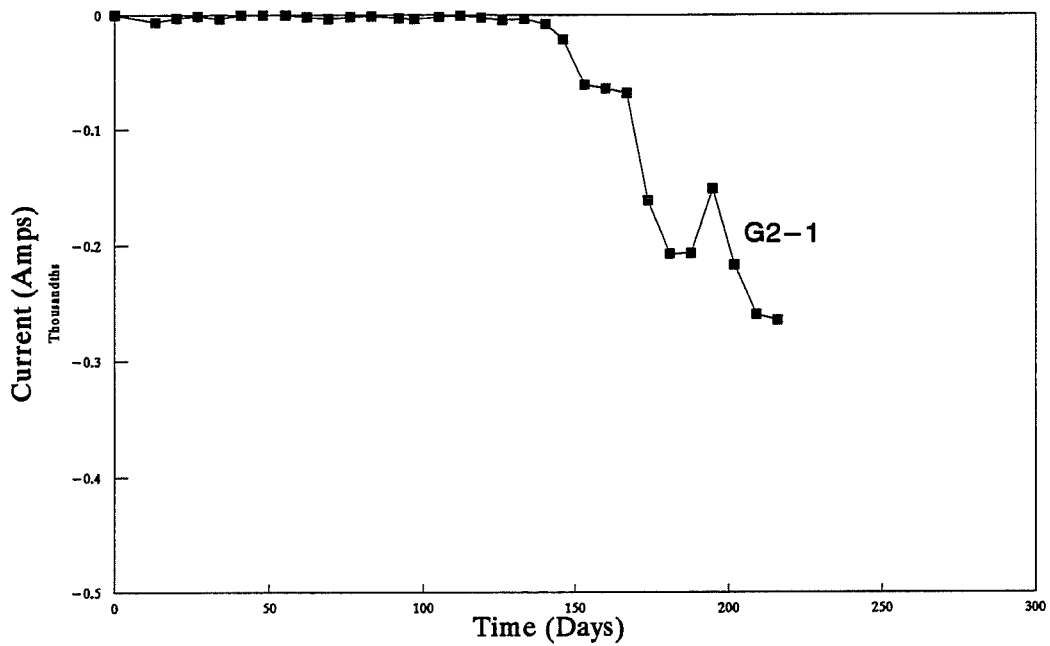
(b) 2 inch Cover

Figure 5.13: Macrocell Tests - Grit Blasted Bars

Figure 5.14: Specimen G1-1

Figure 5.15: Specimen G2-1

5.3 Chloride Concentrations

The chloride content of the macrocells was monitored in time by separate chloride specimens during the exposure period. These results are presented in Appendix B. No attempt has been made to relate the chloride content to the initiation of corrosion since there is extremely high variability in these results. The chloride concentrations and depth profile of one specimen can be drastically different from another specimen; therefore, the results from the chloride specimens do not necessarily correspond with a particular macrocell specimen. The high variability can be seen from the chloride samples that were taken from the autopsy specimens to determine to chloride content at the level of the steel. These chloride results are also given in Appendix B.

Additionally, the results may not accurately reflect chloride concentrations at a given depth of concrete or at the level of the steel since localized samples are taken. The chloride reading is only accurate at the specific location and depth from which the sample was taken. Samples can include aggregate which can give readings that are not representative across the entire specimen at that given depth. Also, the chloride concentration may not be uniform across a constant depth.

5.4 Corrosion Products

Upon opening all specimens, a blackish corrosion product was present. In addition, a small amount of reddish brown product was evident in several cases. After exposure to air, however, the blackish product converted for the most part to a reddish-brown color. From these observations, it appears that the blackish product is black magnetite (Fe_3O_4) which reacts with oxygen to form red-brown iron (III) oxide ($2Fe_2O_3 * H_2O$). These corrosion products,

therefore, indicate that corrosion of steel was evident in all cases. The pitting found in several instances also supports this conclusion.

Since some of the blackish corrosion product did not convert to the reddish-brown color, it is possible that some of the blackish discoloration is from the corrosion of zinc contained in the coating. Zinc can corrode to produce zinc hydroxychloride[15] [$ZnCl_2$ * $4Zn(OH)_2$]. The whitish product of zinc oxide (ZnO) was not apparent in any specimens upon opening.

Since the reddish-brown corrosion product did not form in the concrete in most cases, it is apparent that the oxygen concentration is very low. Low oxygen content could be the reason that zinc oxide was not found.

5.5 Corrosion Locations

Corrosion was found on all bars in the bent region of the bar. Additionally, the corrosion was located from approximately the center of the bar and extended towards the resistor side of the bar as shown in Figure 5.16.

The corrosion may have initiated in the bent region since the steel in this part of the bar has been yielded. Yielded steel in more susceptible to corrosion than non-yielded steel since yielding changes metallurgical properties. Another possibility is that the bent region of all bars except those denoted as "coated" contained new coating from the recoating process while the straight region contained the original coating. There could be a
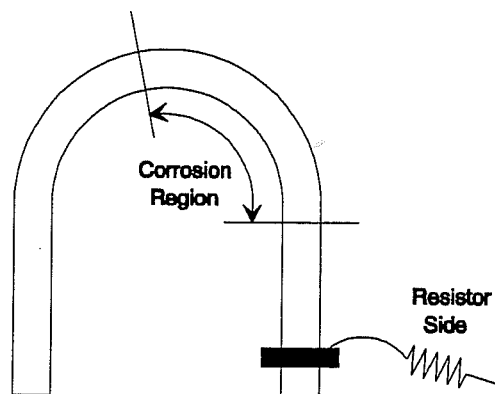

Figure 5.16: Corrosion Locations

difference in corrosion performance because of a difference in the coating or the age of coating.

The corrosion initiated on the resistor side of the bar due to a distance effect. The shortest path for electrons to flow to the cathode is from the resistor side of the bar. The other side is perhaps too electrically distant from the cathode to initiate corrosion in these locations.

5.6 Corrosion Currents

The electrical current is a good indicator of the corrosion occurring on the anode. From the tests conducted and the autopsies that followed, it is apparent that current flow indicates corrosion of the steel. It does not appear that the current is displaying sacrificial action since the corrosion of the steel was evident in all cases even when the bar was examined shortly after the initiation of corrosion current. The current versus time plot also provides the time to initiation of corrosion. As soon as current begins flowing, corrosion has initiated. Further, the current at a given time indicates the instantaneous level of corrosion activity.

The electrical current, however, is not indicative of the total damage that has occurred on the bar. The damage on the bar is proportional to the total number of electrons that have been removed from the anode. The total number of electrons indicate the amount of metal that has been dissociated. By determining the number of electrons that have been removed, it is possible to access the damage (lost metal) that has occurred on the anode. The number of electrons that have been removed can be determined from the area under the current versus time diagram.

The charge flow which indicates the number of electrons removed is plotted versus time for all specimens in Appendix B. The relative damage indicated by these plots corresponds well with the damage observed. The damage level was subjectively rated on a scale from 0 to 10. The ratings were made from visual observations of the damage with 0 indicating no damage and 10 indicating the highest degree of damage seen on any of the bars that were autopsied. The ratings of damage level observed are tabulated along with the measured charge flow in Table 5.1. As can be seen by this comparison, the damage is accurately reflected by the charge flow. Specimens that show similar rankings of damage have measured charge flows that are extremely close. From the values of charge flow, it is obvious that the damage on the one inch specimens was much more severe than on the two inch specimens.

Table 5.1: Damage Level of Macrocell Bar Specimens		
Specimen	Charge Flow (C)	Visual Rating (0-10)*
G1-1	3678	10
C1-2	3431	10
R1-2	2857	9
D1-2	2539	8
R2-2	1061	4
G2-1	1047	3
D2-1	996	3
C2-3	111	1

* 0 - No Damage   10 - Highest Degree of Damage of the 8 Specimens

5.7 Corrosion Environments

There is a drastic difference in corrosion performance of coated reinforcing steel placed in concrete and that exposed to air. All coated specimens except the bars that had bending damage (Coated) in the air exposure tests performed excellently. No visual signs of steel corrosion were evident. In the macrocell specimens, however, corrosion of steel was evident in all cases.

There are two possible reasons for the difference in performance noted. First, it appears that the coating is chemically altered by the concrete. During hydration, the concrete may react with the coating to render the coating essentially ineffective. It seems highly likely that the calcium in the cement attacks the silicate in the coating to produce calcium silicate. This theory is supported by the fact that the coating is removed from the bar and remains attached to the concrete. The coating that remains on the concrete is in a grey powder form indicating that the silicate has probably been removed from the coating. Further, there is a possibility that the coating is affected by the high alkalinity created by the cement in the concrete.

Another reason for differences noted in the tests is that the air exposure tests are microcell corrosion tests while the concrete tests are macrocells. The microcells can develop anodes on only part of the bar while the rest remains cathodic. In the macrocell tests, however, the entire bar becomes anodic which provides a higher probability that a part of the bar will corrode.

5.8 Corrosion Protection in Concrete

The high ratio zinc silicate coating tested did not protect the steel from corrosion. There does not seem to be any difference between coating

methods or damage levels. Steel corrosion was evident in all cases, and the corrosion currents and damage appear to be similar.

It is highly probable that the coating in concrete experiences chemical reactions along with the concrete during hydration. Corrosion occurred in all cases regardless of damage. In addition, the bent region of the bar (yielded steel) was attacked preferentially over the unyielded steel. Finally, the corrosion rates and damage levels of the coated steel are similar to the black bars. These factors indicate that corrosion occurred as if the coating was not present.

From the tests performed on different concrete covers, it is obvious that additional concrete cover can delay the initiation of corrosion. This method of corrosion protection can increase the life of a structure, but is not considered a method of preventing corrosion.

CHAPTER 6
SUMMARY AND CONCLUSIONS

6.1 Introduction

Corrosion of reinforcing steel in concrete is a problem that threatens the integrity of structures and shortens their service life. Corrosion can be prevented or reduced by the application of coatings. Coatings, however, can lead to structural problems since they can reduce bond and bond strength.

A high ratio zinc silicate coating has been proposed to prevent the corrosion of reinforcing steel. The objectives of this study, therefore, were to evaluate the corrosion protection afforded by the coating in a concrete corrosion environment and to evaluate the structural performance of the coated reinforcement.

6.2 Structural Bond Tests

Eight beams were tested to determine the influence of a high ratio zinc silicate coating on bond. The beams were tested in negative bending with the reinforcement lapped spliced in a constant moment region. Companion coated and uncoated specimens were tested with variables that included concrete cover, bar spacing, and bar size. All specimens failed by splitting in the splice region before reaching yield in the steel.

The following conclusions were made:

1)   The load-deflection characteristics were not affected by the coating.

2)   The crack widths and crack distributions were not significantly affected by the coating.

3)   The bond strength was not affected by the coating.

71

Current structural provisions governing development lengths for uncoated bars can be used when designing structural members containing reinforcing steel coated with a high ratio zinc silicate.

6.3 Corrosion Tests

Twenty four macrocell specimens were tested to evaluate the corrosion protection afforded by a high ratio zinc silicate. The concrete macrocell specimens were subjected to a cyclic exposure of chloride solution over a period of approximately 7 months. Variables tested included concrete cover, coating damage, and recoating application methods. In addition, ten air exposure specimens were subjected to a cyclic exposure of chloride solution.

The following conclusions were made:

1) Steel corrosion was experienced on all macrocell specimens regardless of coating condition or damage level.

2) Electrical current indicated the initiation of corrosion. In addition, the total damage that occurred on the bar could be determined from the charge flow.

3) A concrete environment is dramatically different from an atmospheric environment. The concrete environment adversely affected the particular coating used. The concrete probably reacted with the coating to decrease or eliminate the corrosion protection afforded by the coating.

The particular formulation of high ratio zinc silicate used for this study was not adequate for corrosion protection of reinforcing steel in concrete. A different formulation will be needed to provide a coating suitable for use in a concrete environment.

Appendix A

Structural Bond Test Data

74

Table A.1: Lap-Splice Test Data

Specimen	f_c (psi)	l_s (in)	Side	Top	Spacing	Top	Spacing	Top	Side	P_{max} (kips)	f_{su} (ksi)
						Covers and Spacings (Nearest 16th of an inch)					
B1-6	4730	18	1.625	1.500	0.875	1.438	0.875	1.438	1.625	15.9	45.7
C1-6	4730	18	1.500	1.313	0.938	1.313	0.938	1.375	1.500	15.9	45.7
B1-11	4730	36	2.125	2.000	3.625	1.938	4.250	1.938	1.875	35.7	43.6
C1-11	4730	36	1.625	2.063	4.000	2.125	4.000	2.063	1.813	37.1	45.3
B2-6	3820	18	1.063	1.000	3.750	1.000	3.875	1.000	1.000	17.5	47.8
C2-6	3820	18	1.063	1.000	3.813	0.938	3.875	1.000	1.063	16.5	45.0
B2-11	3820	36	2.000	2.250	1.125	2.250	1.250	2.250	2.000	27.8	34.8
C2-11	3820	36	2.188	2.250	1.250	2.250	1.375	2.250	2.250	27.5	34.4
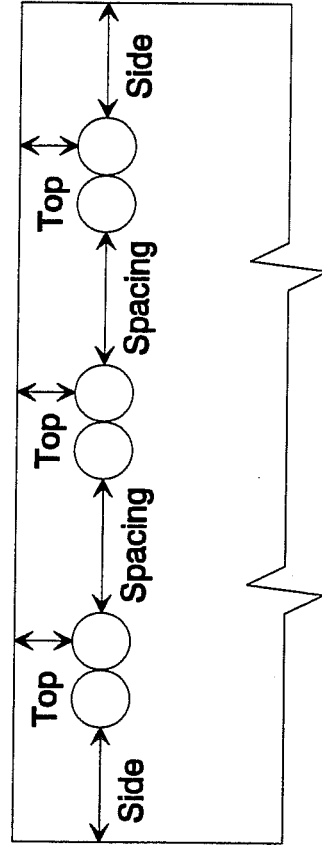
Appendix B

Corrosion Test Data

Table B.1: Chloride Concentration of Chloride Specimens* (% Weight of Concrete)					
Sample Depth (in)	Days of Exposure				
	76	115	139	169	228
0.25 - 0.5	0.31	0.39	0.32	0.39	0.35
0.75 - 1.0	0.20	0.25	0.26	0.18	0.19
1.25 - 1.5	0.15	0.18	0.17	0.15	0.14
1.75 - 2.0	0.09	0.11	0.10	0.10	0.08
2.25 - 2.5	0.07	0.08	0.07	0.03	0.03
2.75 - 3.0	-	-	0.07	0.01	0.01

* Average of 2 samples

Table B.2: Chloride Concentration of Macrocell Specimens [*]
(% Weight of Concrete)

Sample Depth (in)	Specimen									
	C1-2	C2-3	R1-2	R2-2	D1-2	D2-1	G1-1	G2-1
0.25 – 0.5	0.23	0.32	0.46	0.44	0.41	0.39	0.73	0.58
0.75 – 1.0	0.28	0.17	0.33	0.28	0.33	0.28	0.40	0.40
1.25 – 1.5	0.20	0.14	0.29	0.20	0.28	0.24	0.36	0.30
1.75 – 2.0	0.25	0.13	0.15	0.16	0.23	0.17	0.28	0.16
2.25 – 2.5	0.19	0.04	0.25	0.16	0.14	0.14	0.22	0.09

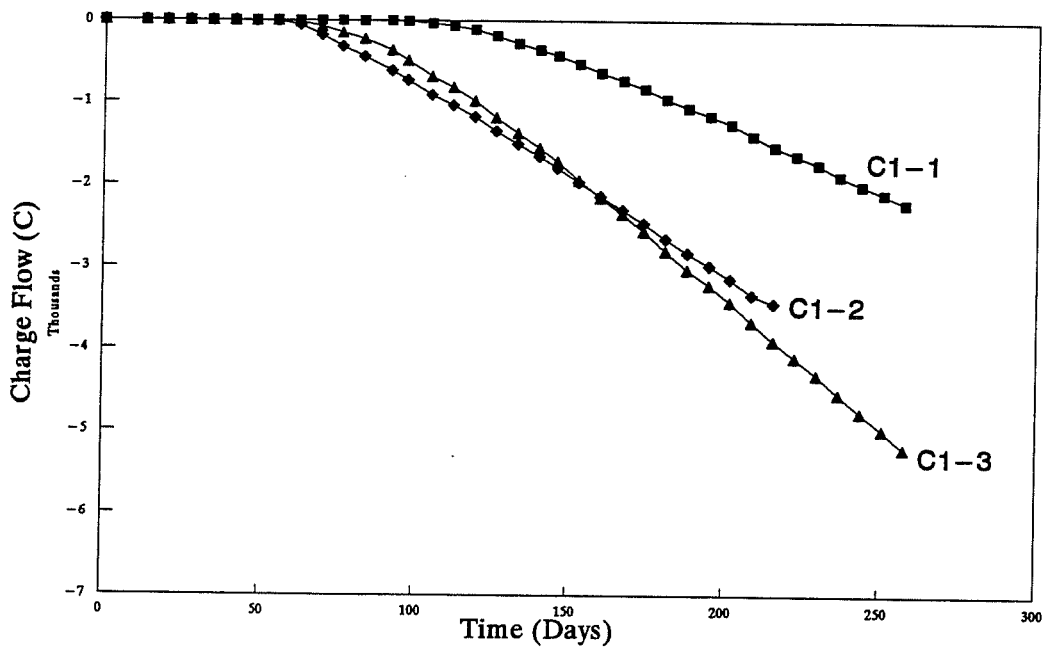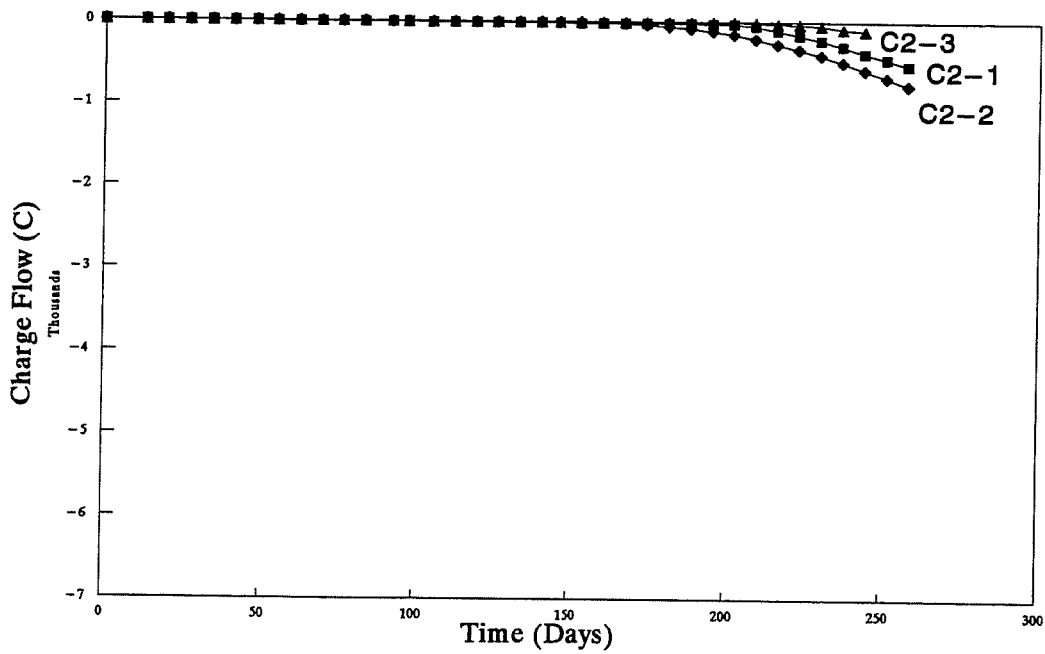[*] Average of 2 samples at the end of the exposure period
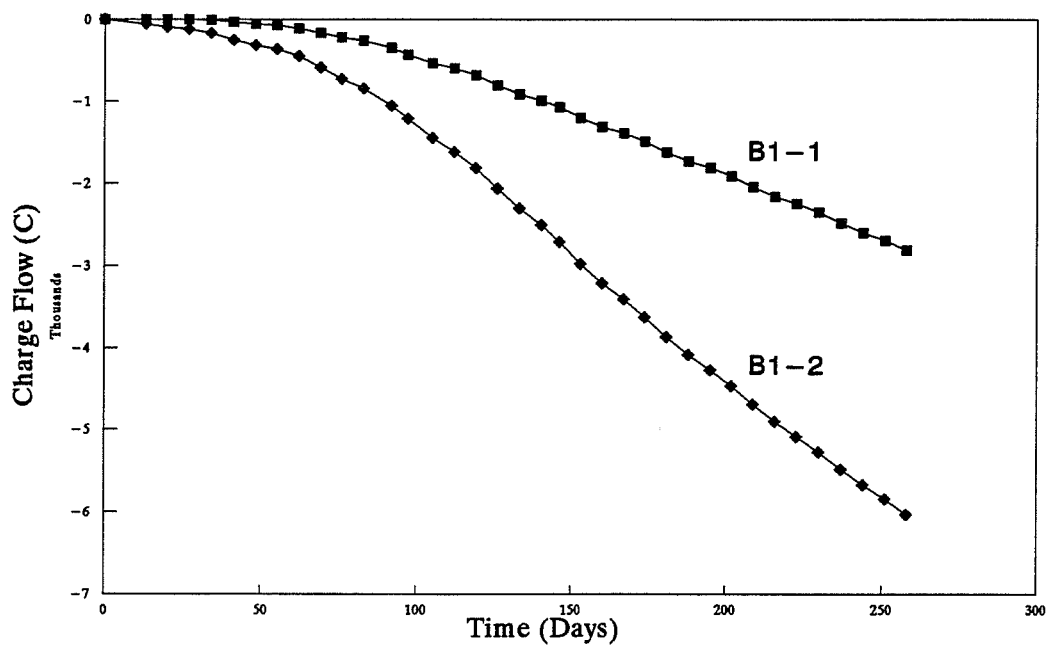
(a) 1 inch Cover
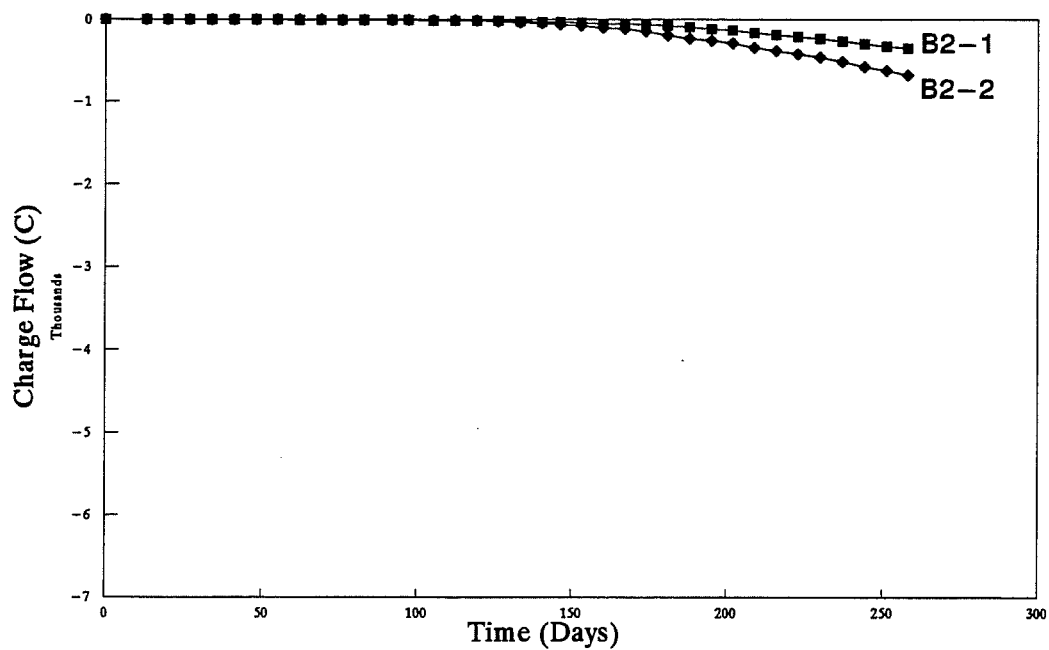
(b) 2 inch Cover

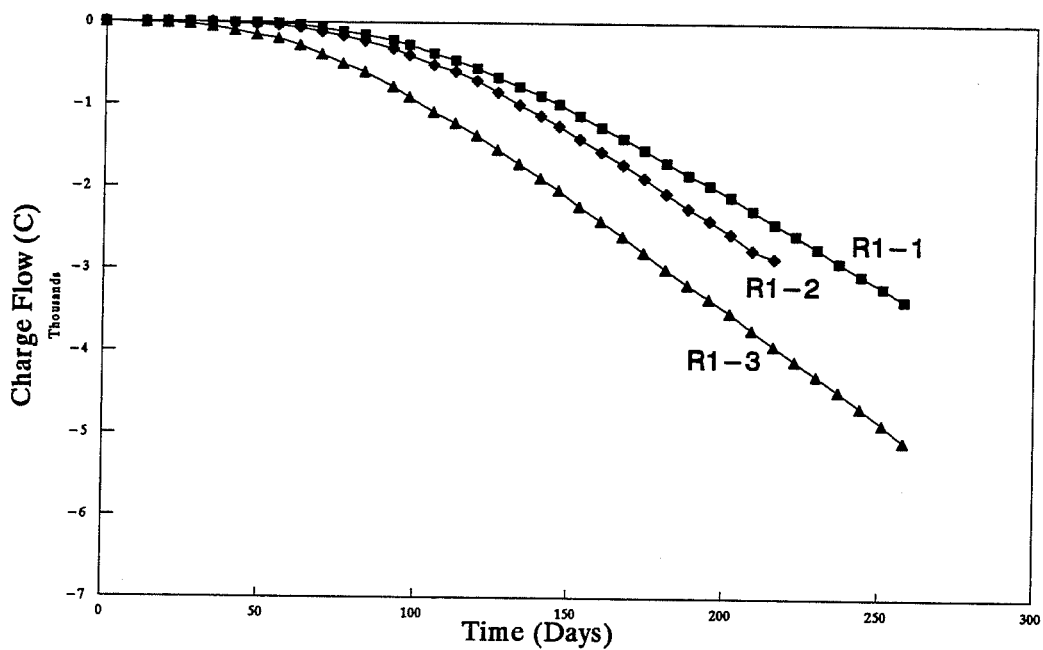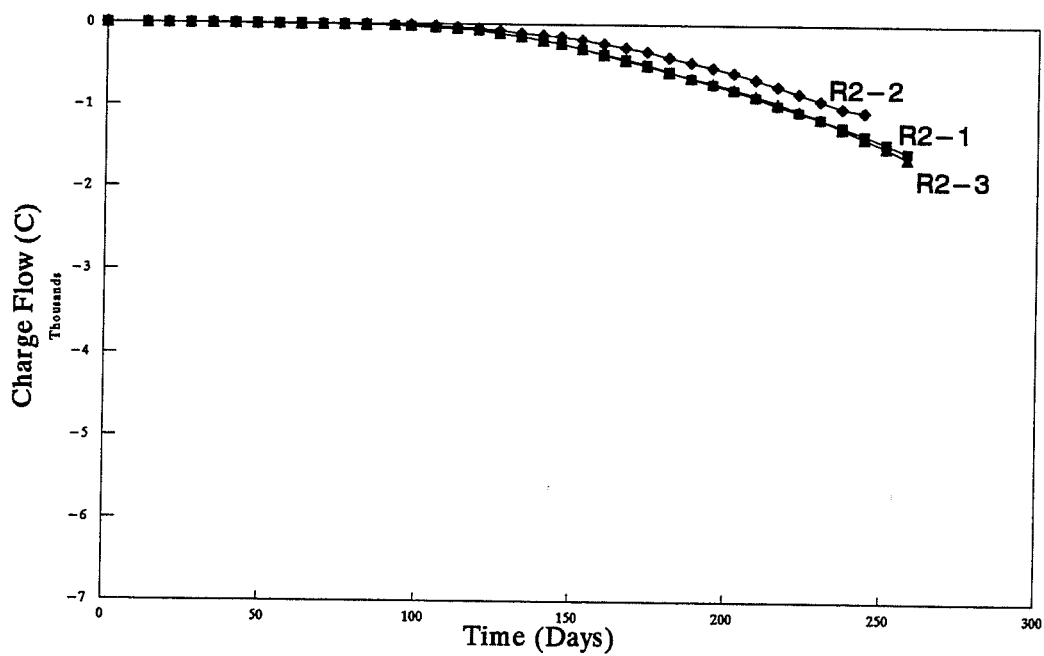Figure B.1: Macrocell Tests - Black Bars

(a) 1 inch Cover

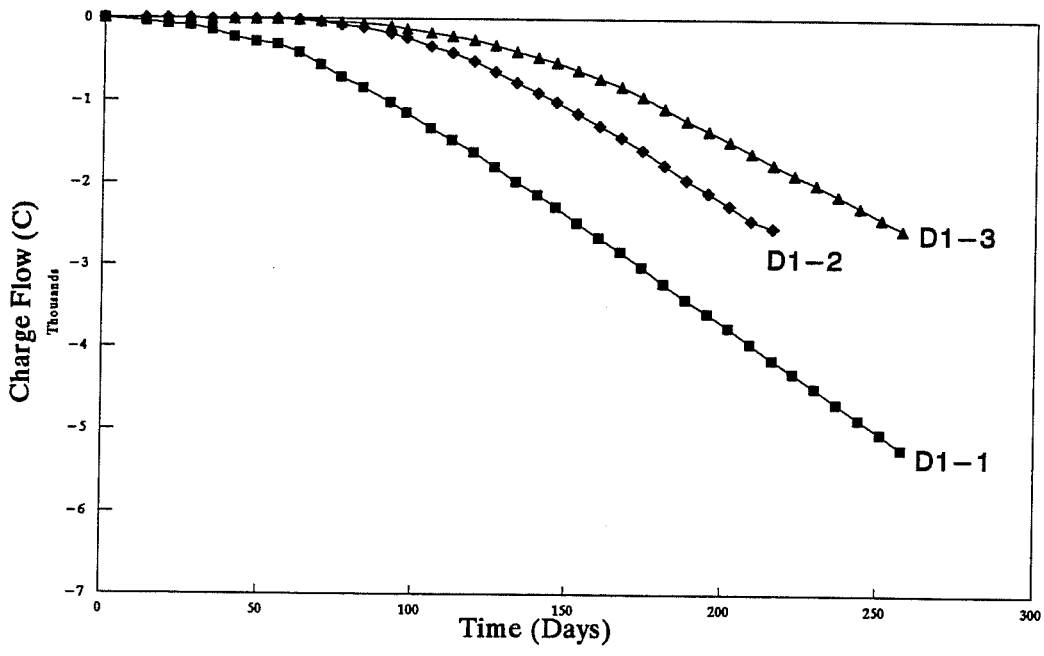(b) 2 inch Cover

Figure B.2: Macrocell Tests - Coated Bars
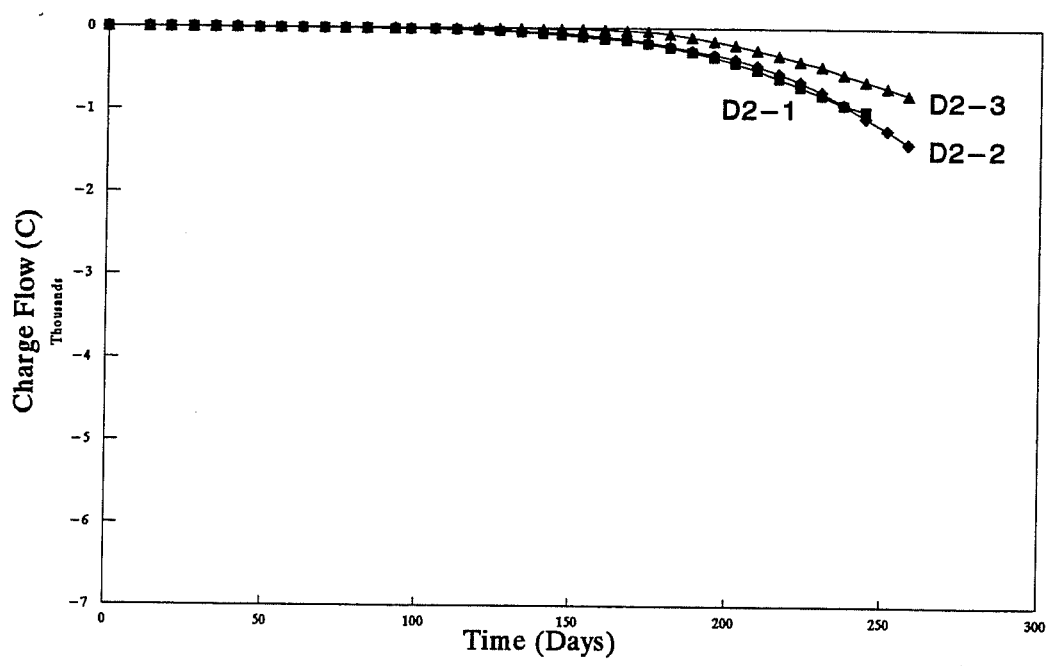
(a) 1 inch Cover

(b) 2 inch Cover

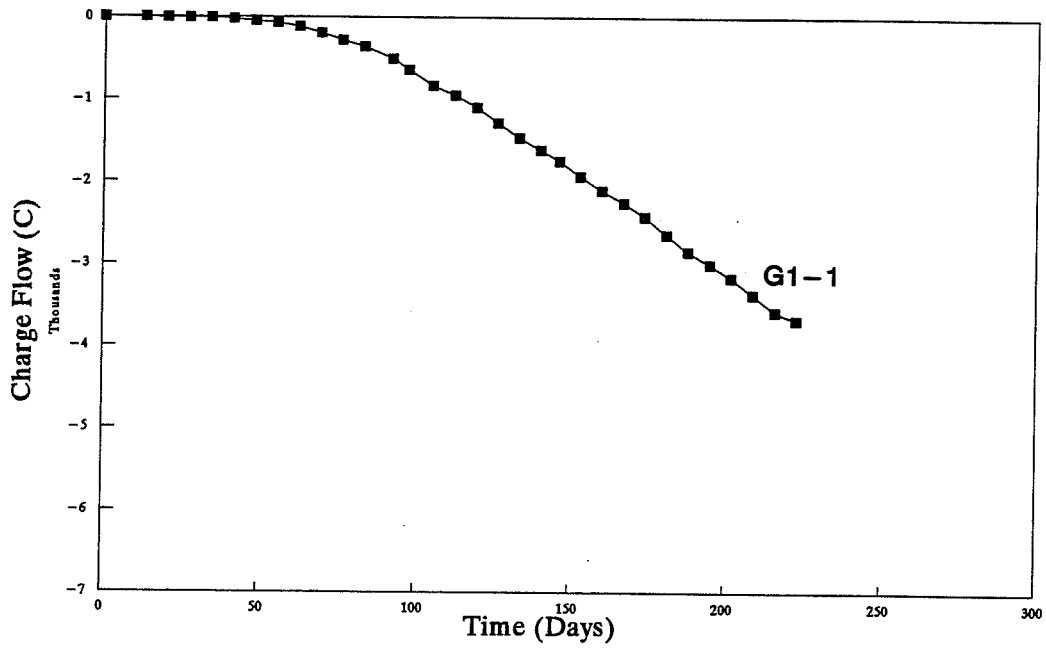**Figure B.3: Macrocell Tests - Recoated Bars**
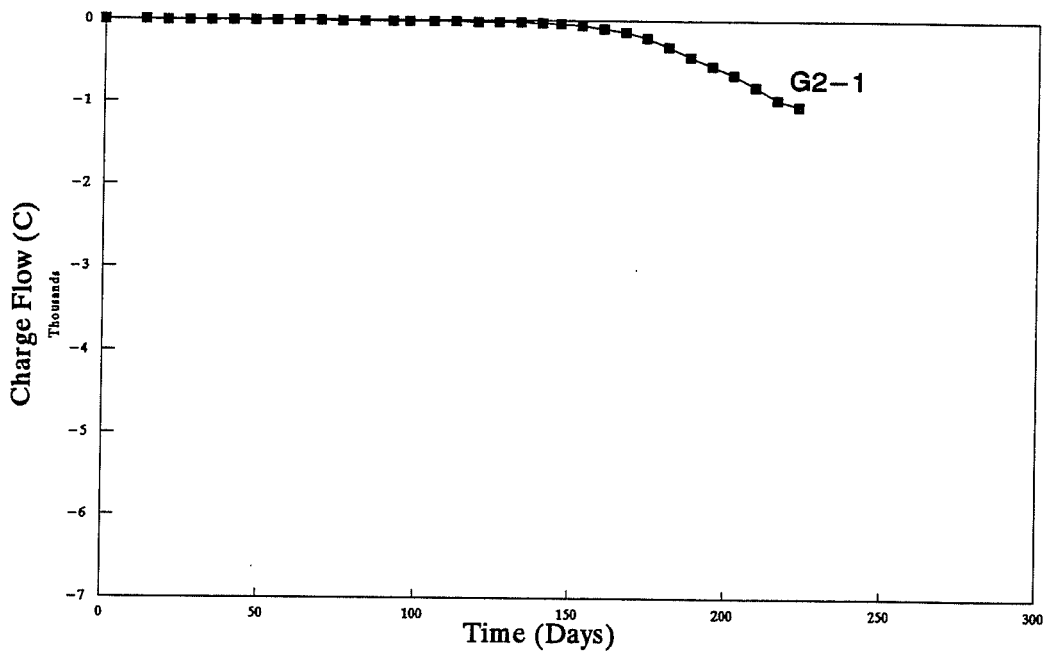
(a) 1 inch Cover

(b) 2 inch Cover

Figure B.4: Macrocell Tests - Damaged Bars

(a) 1 inch Cover

(b) 2 inch Cover

Figure B.5: Macrocell Tests - Grit Blasted Bars

BIBLIOGRAPHY

1. ACI Committee 318, "Building Code Requirements for Reinforced Concrete and Commentary," ACI Standard 318-89, American Concrete Institute, Detroit, 1989.

2. AASHTO, Standard Specification for Highway Bridges (Fourteenth Edition), American Association of State Highway and Traffic Officials, Washington, D.C., 1989.

3. CEB, "Protection Systems for Reinforcement, Comite Euro-International Du Beton, Bulletin D'Information No. 211, February 1992.

4. Clear, K.C. "Effectiveness of Epoxy Coated Reinforcing Steel," Concrete International, May 1992, pp. 58-64. See CRSI Comments, same edition.

5. Clear, K.C., "Time to Corrosion of Reinforcing Steel in Concrete Slabs, V. 4: Galvanized Reinforcing Steel," Report No. FHWA/RD-82/028, Federal Highway Administration, Washington, D.C., December 1981.

6. Clear, K.C., and Virmani, Y.P., "Solving Rebar Corrosion Problems in Concrete Research Update: Methods and Materials," NACE.

7. Cornet, I., and Bresler, B., "Corrosion of Steel and Galvanized Steel in Concrete," Materials Protection, April 1966, pp. 69-72.

8. Delahunt, J.F., and Nakachi, N., "Long Term Economic Protection with One-Coat of Inorganic Zinc-Rich," Journal of Protective Coatings and Linings, February 1989, pp. 48-53.

9. Fontana, M.G., Corrosion Engineering, McGraw Hill, Inc., 1986.

10. Hamad, B.S., "Effect of Epoxy Coating on Bond and Anchorage of Reinforcement in Concrete Structures, Ph.D. Dissertation, Department of Civil Engineering, The University of Texas at Austin, December 1990.

11. Kotc, J.C., and Purcell, K.F., <u>Chemistry & Chemical Reactivity</u>, CBS College Publishing, 1987.

12. Munger, C.G., "Inorganic Zinc Coatings: A Review," Journal of Protective Coatings and Linings, June 1987, pp. 187-193.

13. Munger, C.G. "VOC-Compliant Inorganic Zinc Coatings," Materials Protection, October 1990.

14. Orangun, C.O., Jirsa, J.O., and Breen, J.E., "A Reevaluation of Test Data on Development Length and Splice," ACI Journal, March 1977, pp. 114-122.

15. Pfeifer, D.W., Landgren, R., and Zoob, A., "Protective Systems for New Prestressed and Substructure Concrete," Report No. FHWA/RD-86/193, Federal Highway Administration, Washington, D.C., April 1987.

16. Szokolik, A., "Evaluating Single-Coat Inorganic Zinc Silicates for Oil and Gas Production Facilities in Marine Environments," Journal of Protective Coatings and Linings, March 1992, pp. 22-43.

17. Treece, R.A. , "Bond Strength of Epoxy-Coated Reinforcing Bars," Master's Thesis, Department of Civil Engineering, The University of Texas at Austin, May 1987. See also ACI Materials Journal, March-April 1989.

VITA

Robert Joseph Frosch was born in New Orleans, Louisiana, on May 1, 1969, the son of Bessie Gagliano Frosch and Warren Robert Frosch, Jr. After graduating Summa Cum Laude from Holy Cross High School, New Orleans, Louisiana, in 1987; he entered Tulane University in New Orleans, Louisiana. He graduated in May, 1991, as valedictorian of the School of Engineering receiving the degree of Bachelor of Science in Engineering, Summa Cum Laude with Departmental Honors. In September, 1991, he entered the Graduate School of the University of Texas at Austin. He is the recipient of the Engineering Foundation Graduate Fellowship, the Engineering Foundation Endowed Presidential Graduate Scholarship, and the John E. Breen Endowed Presidential Scholarship. He has worked at the University of Texas at Austin as a Teaching Assistant and as a Graduate Research Assistant at the Phil M. Ferguson Structural Engineering Laboratory. In addition, he has worked for Modjeski and Masters Consulting Engineers as an Engineering Technician and an Engineer-in-Training.

Permanent Address: 3220 Duval Road #1506
                      Austin, Texas 78759

This thesis was typed by the author.